19TH INTERNATIONAL CONFERENCE & EXHIBITION ON DEVICE PACKAGING
FOUNTAIN HILLS, AZ • WWW.DEVICEPACKAGING.ORG • MARCH 13-16, 2023

# 4D mmW/5G Metasurfaces and Wireless Sensors combining additive manufacturing, morphing and ML technologies

K.Hu and M.M.Tentzeris

Georgia Institute of Technology

ATHENA

# Additive Manufacturing Technologies: A Manufacturing Revolution

Additive Manufacturing technologies

Inkjet Printing

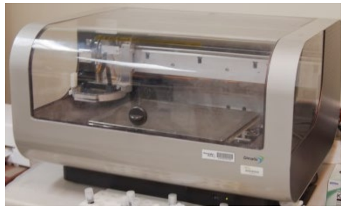

3D Printing

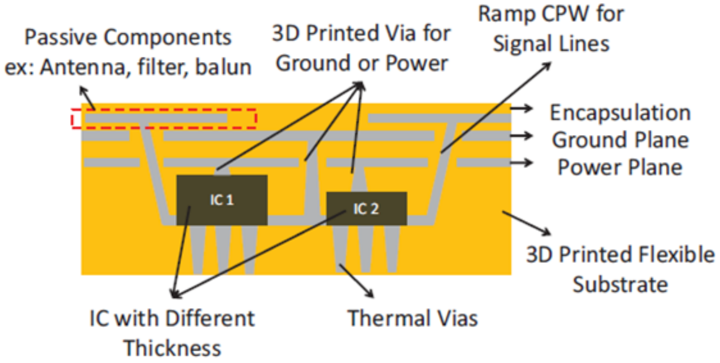


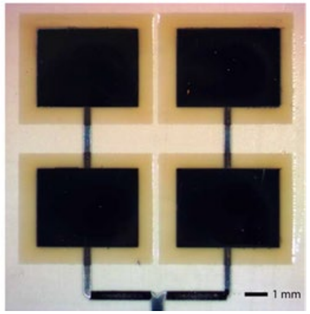


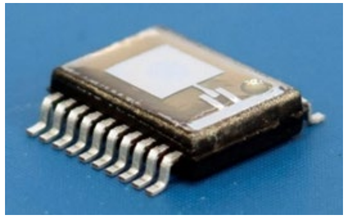

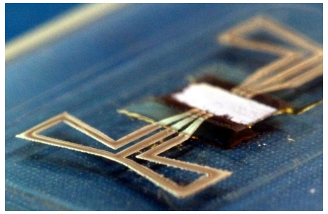


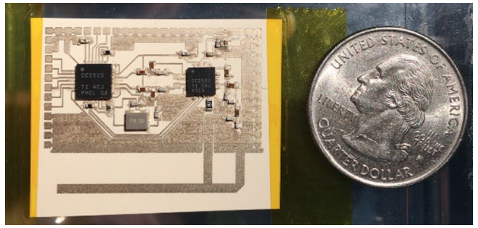

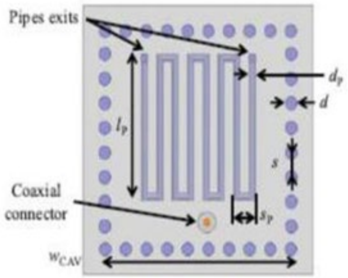


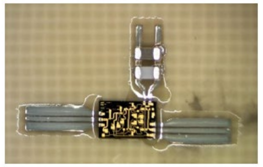

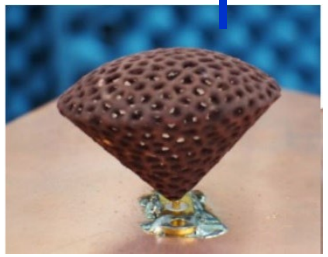

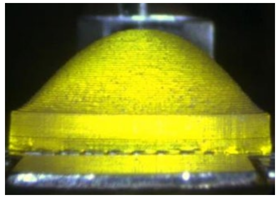

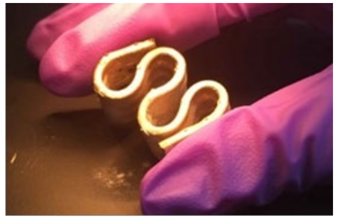

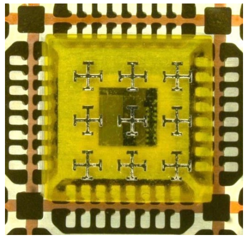

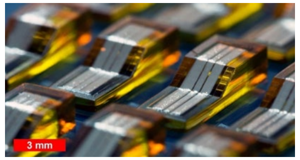


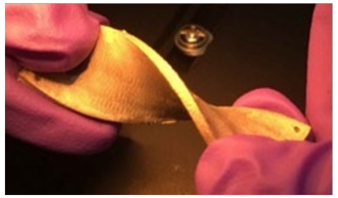

# The First Fully Printed Autonomous Wireless Modules (IoT/5G)

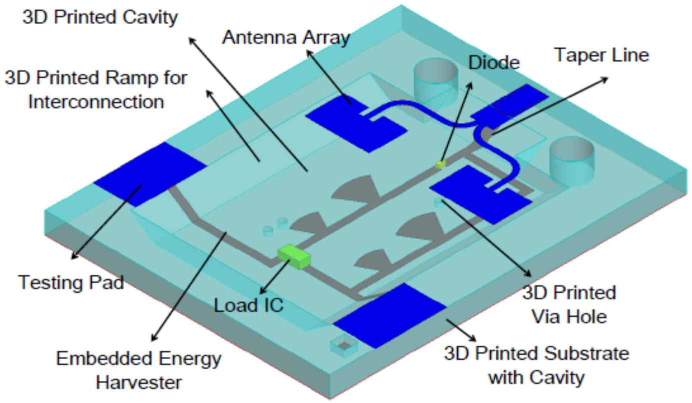


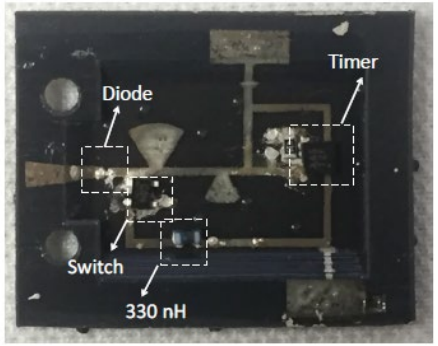


28GHz Backscatter RFID-enabled Sensing 5G/IoT module

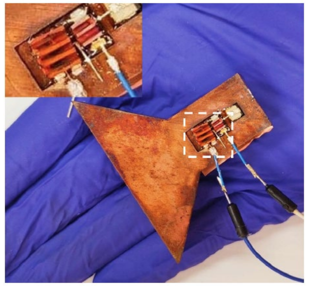

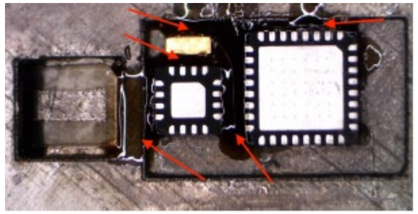

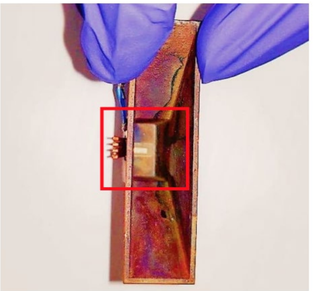

12-18 GHz Tunable System-on-Antenna for IoT

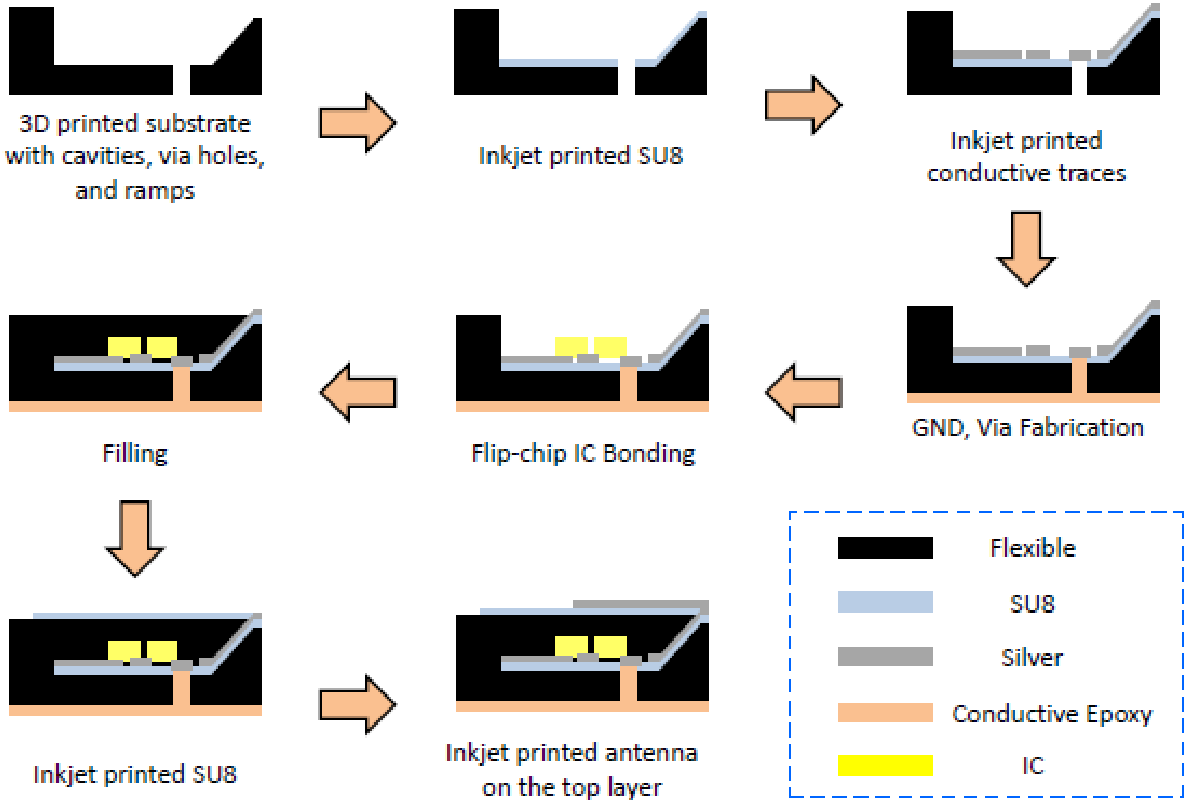

# Fully Printable Rugged Conformal Interconnects up to mmW/sub-THz

## Printed 3D RF Interconnects

- Goal: mitigate losses from bond wires/ribbons and package transitions for MMIC devices
- Surface mount
  - MMIC die bonded to PCB
  - Dielectric ink printed to form 3D ramps up to surface of die
  - Metallic ink printed to pattern interconnects from PCB to die
- Cavity-embedded
  - MMIC die bonded to GND of cavity within PCB
  - Dielectric ink printed to fill gaps between die and PCB
  - Metallic ink printed to pattern transitions from PCB to die across printed gap fills

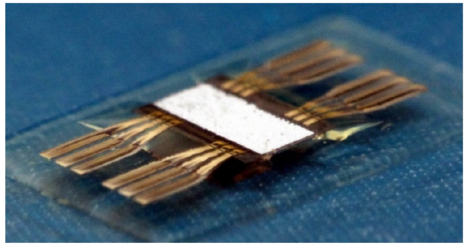

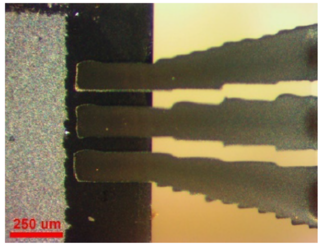



Side-view schematic of surface mount scenario

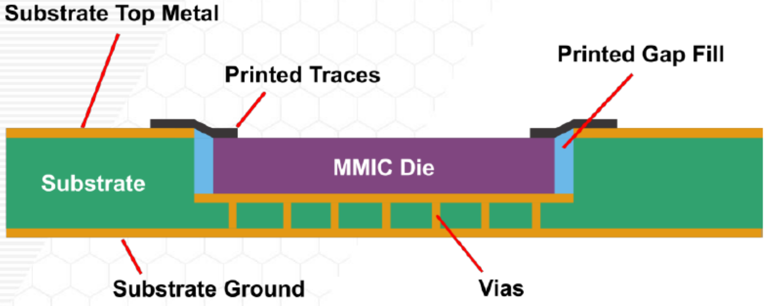


Side-view schematic of cavity-embedded scenario

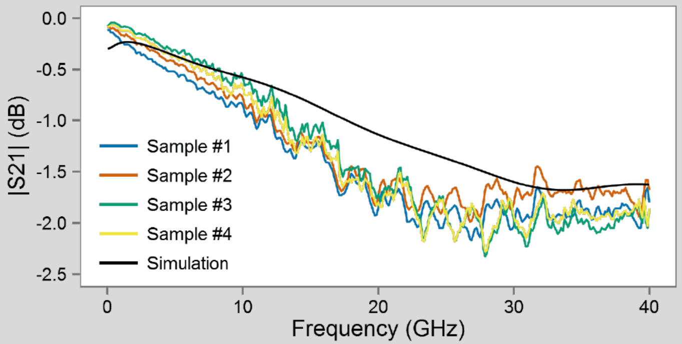


- Loss at 40 GHz: **0.6–0.8 dB/mm**
- Inductance **half** of typical wirebond (0.4 nH/mm)

Efficient interconnects essential for system-on-package (SoP) solutions

# Fully Additively Manufactured Self-Monitoring MultiChip Modules (MCM)

FEM MCM Includes PA LNA and Switch MMICs integrated onto printed “intelligent” (EMI Suppressing/ self monitoring) package

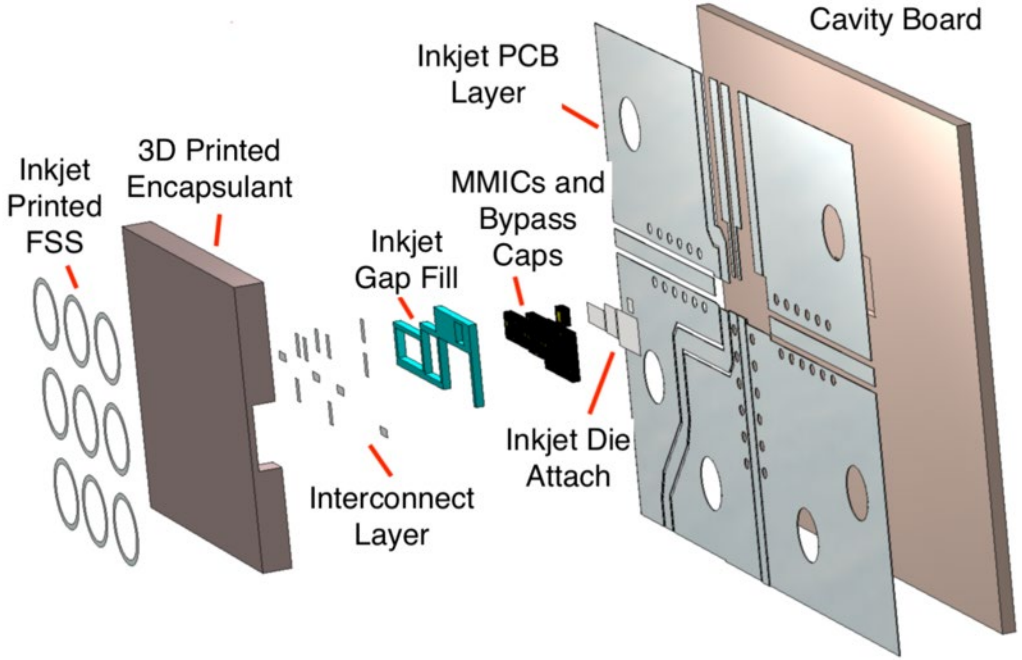


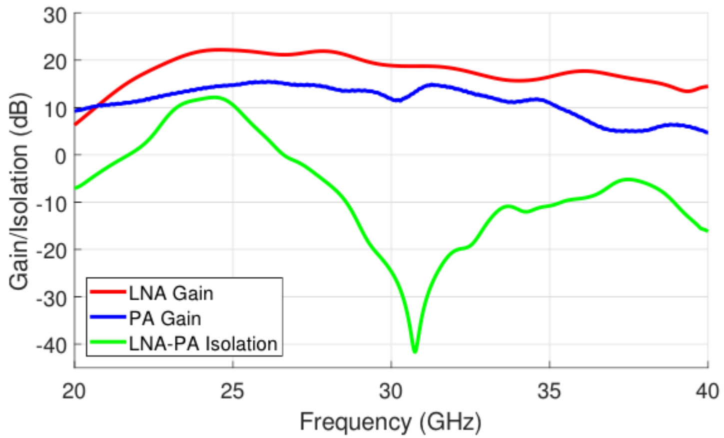


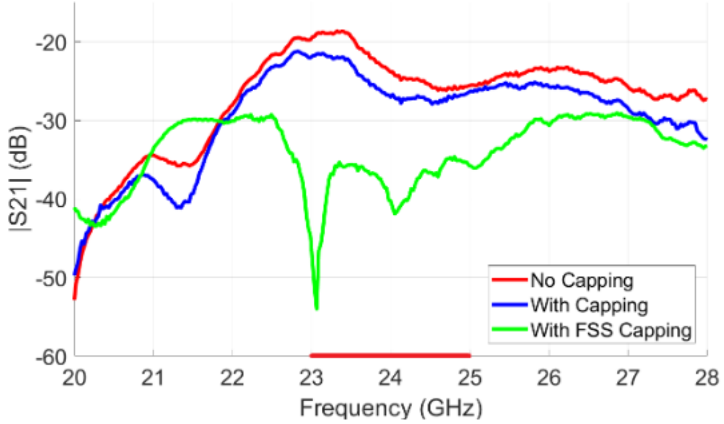


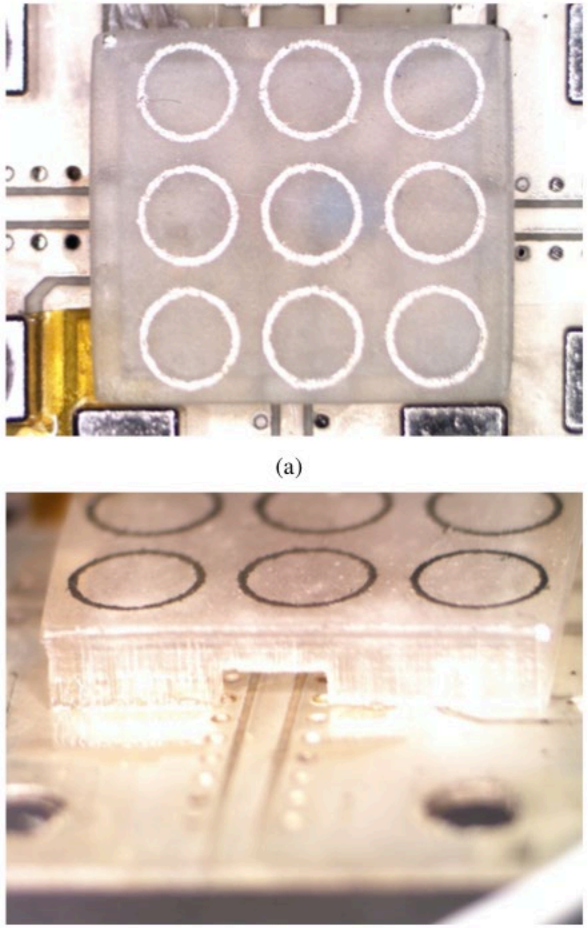
(a)

(b)

# System On Antenna (SOA)

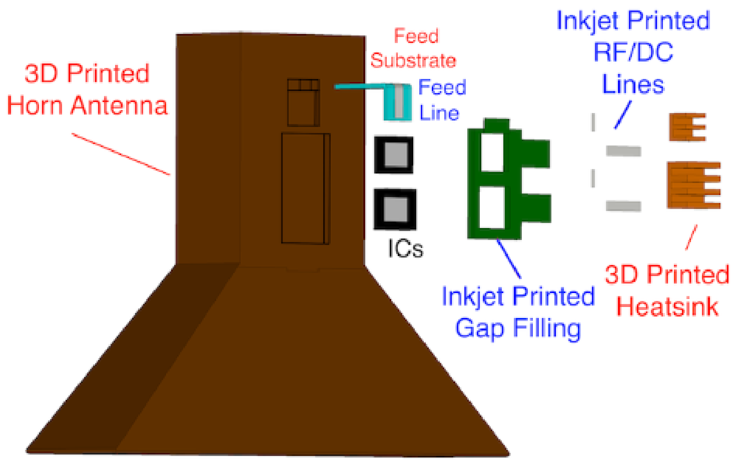


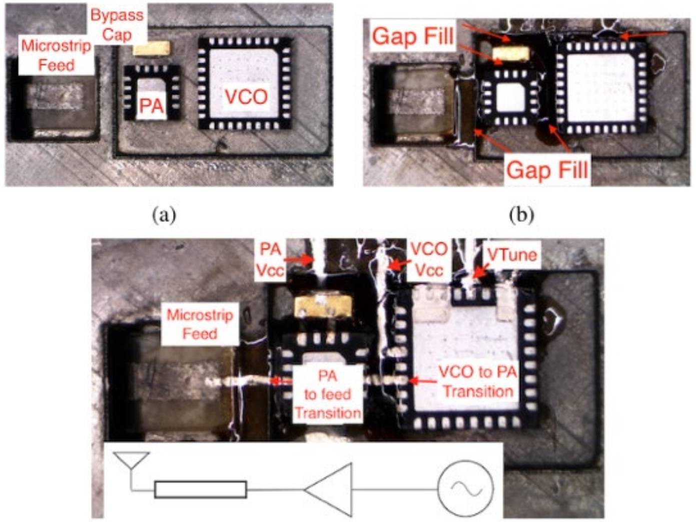

(a) (b) (c)

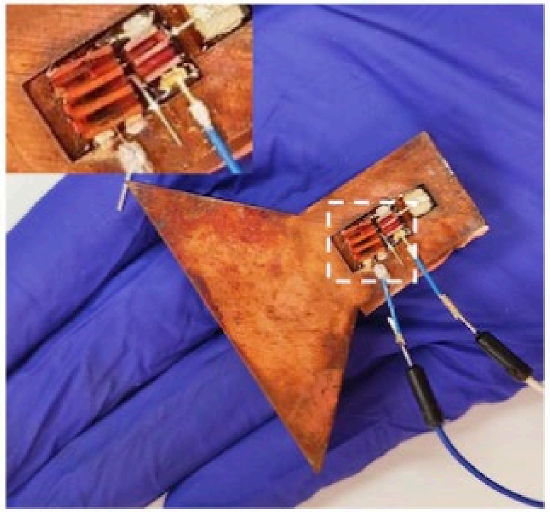
(a)

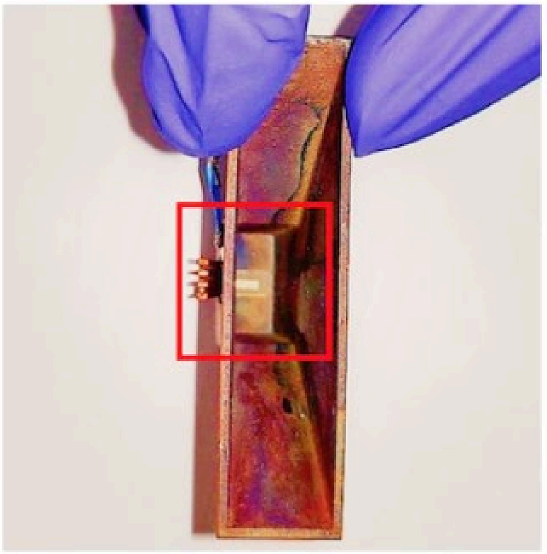

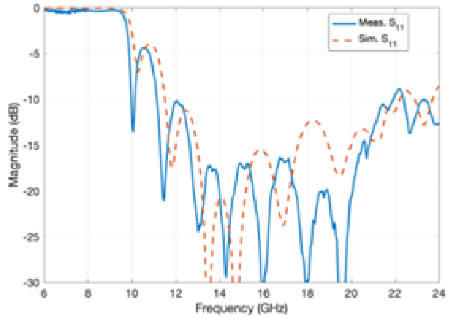


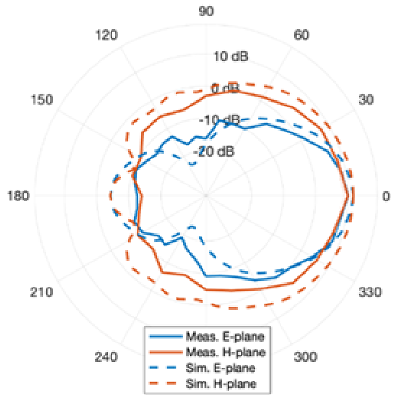


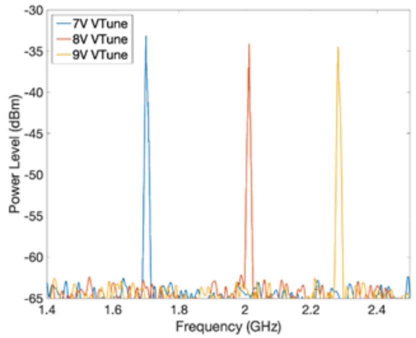

# Camera-inspired 3D Lens-based mmID: wide interrogation angle for "agnostic" wireless links

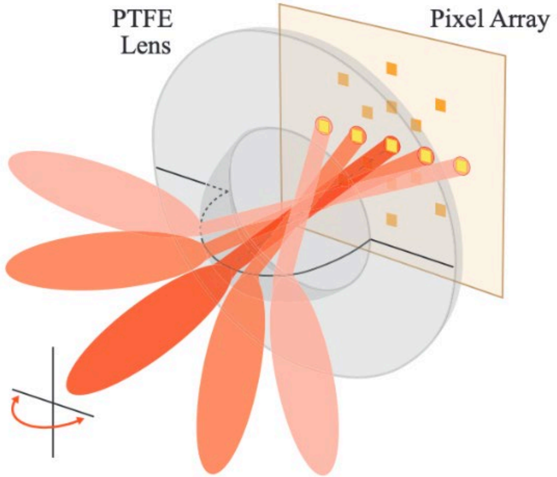


Provides retro-directive behavior through focalizing on the RF 'pixels'.

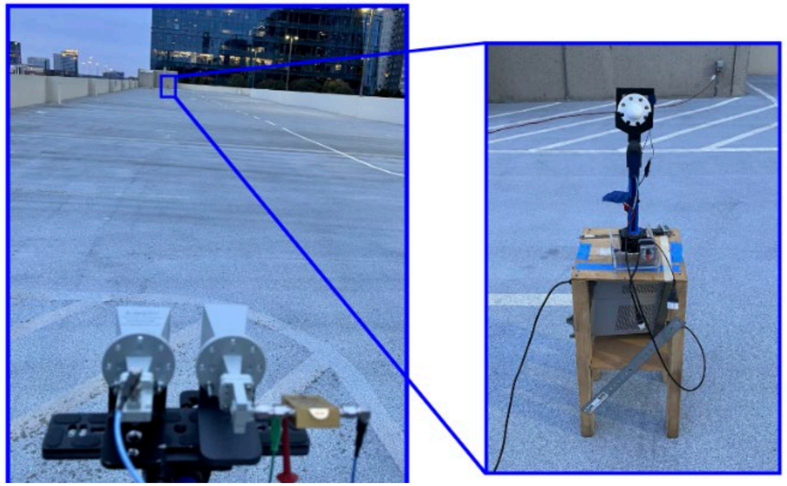

Interrogation experimental setup at 80 m.

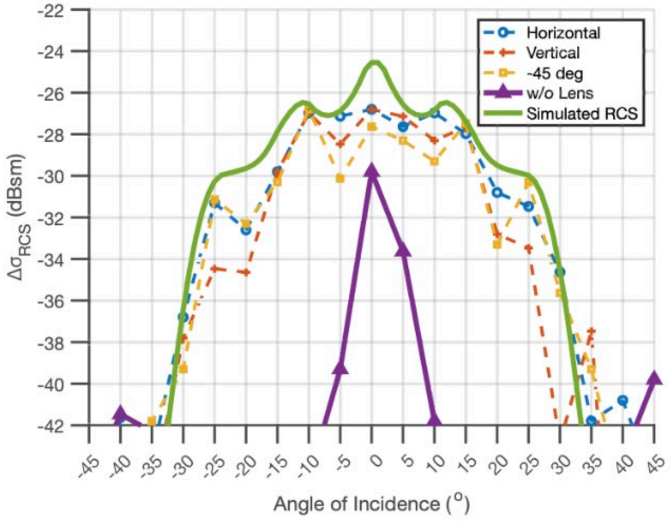


Broad solid angular coverage up to $\pm 28°$ **of -10 dB beamwidth.**

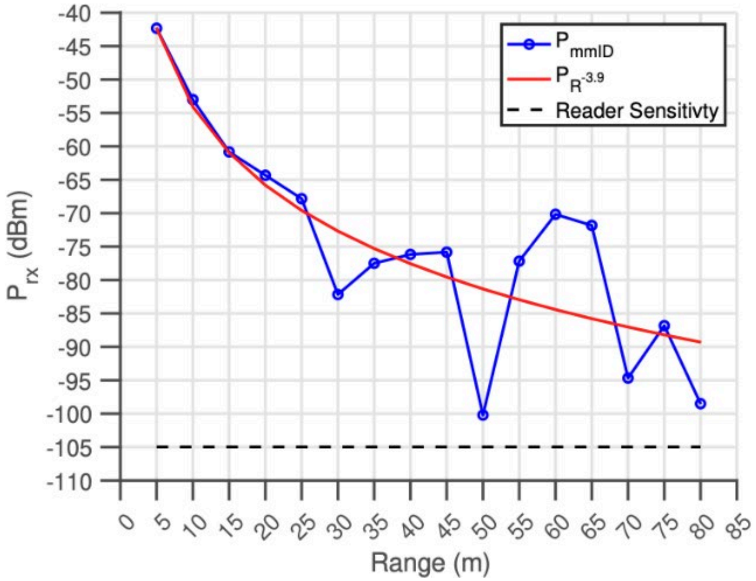


**Interrogated up to 80 m** away with a proof-of-concept reader.


ATHENA Georgia Tech

# Cascaded 3D Lens-based mmID: even wider angular coverage

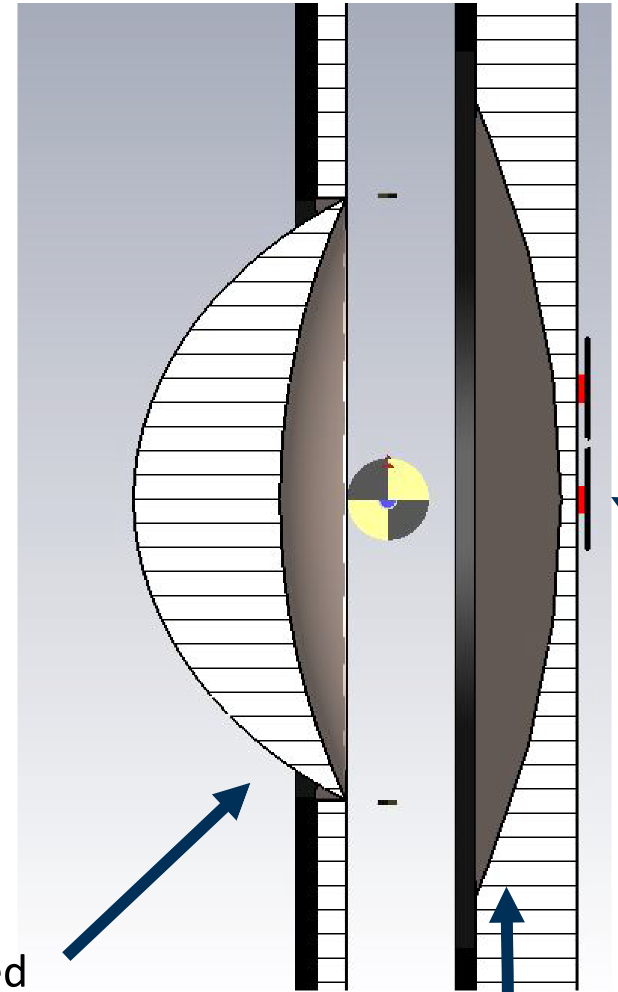


Through cascading multiple lenses, overcoming the gain/angular coverage trade-off is enabled.

Solid angular coverage increases to $\pm 40°$, while being within **1 dB** of peak gain of the single lens-based mmID.

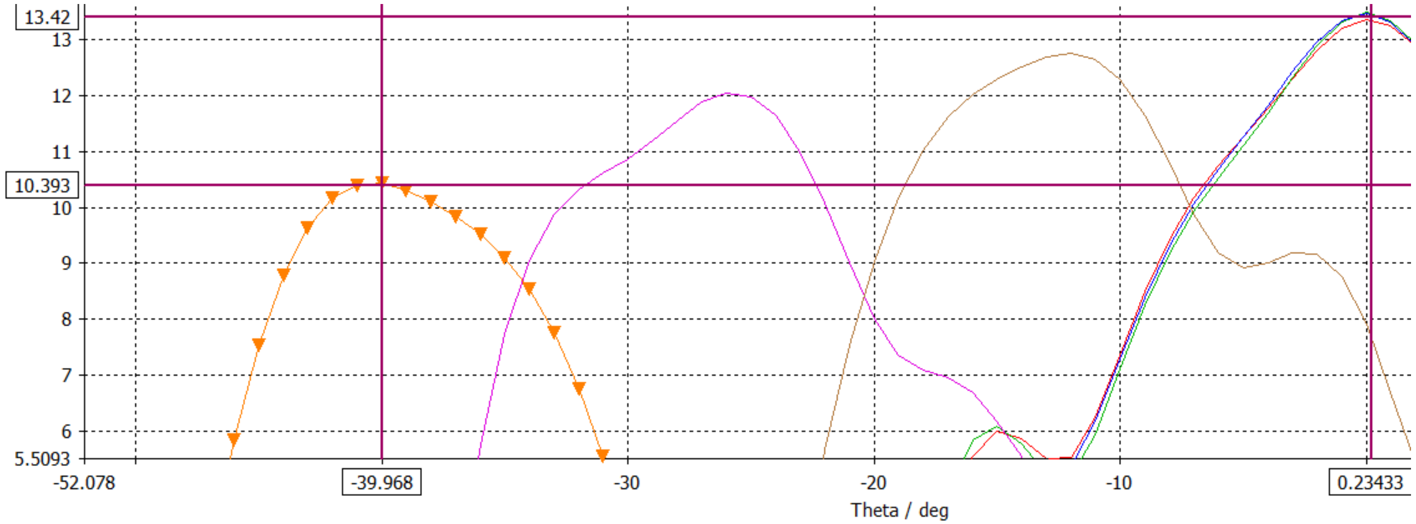

# 4-DOF “Eggbox” Origami FSS

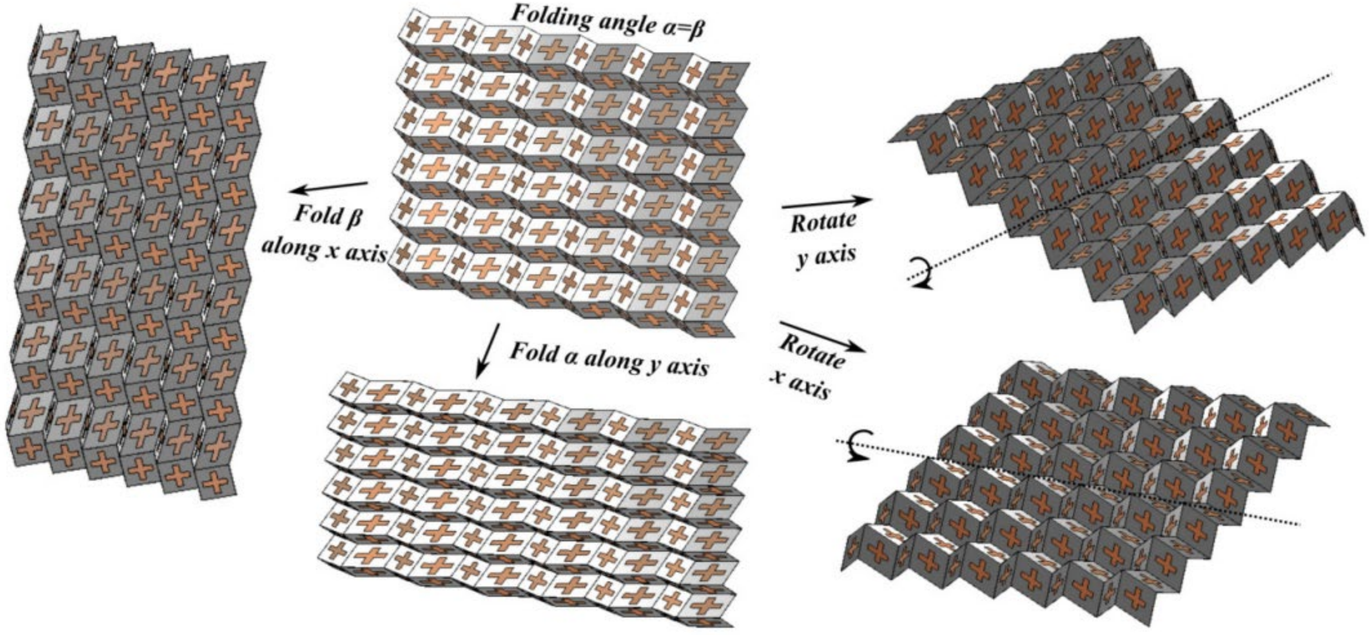


**6x6 cross-dipole Eggbox FSS**

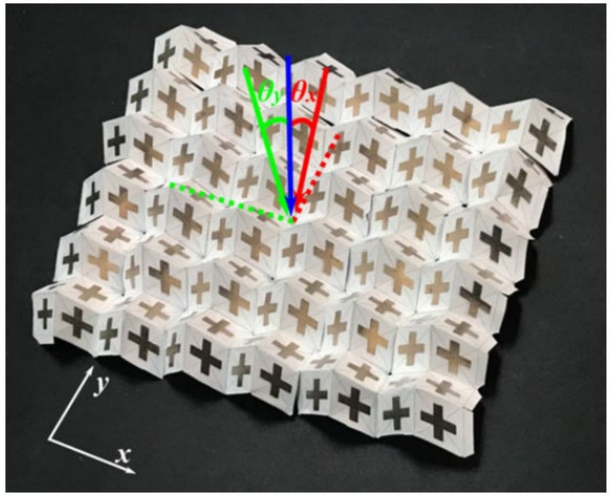


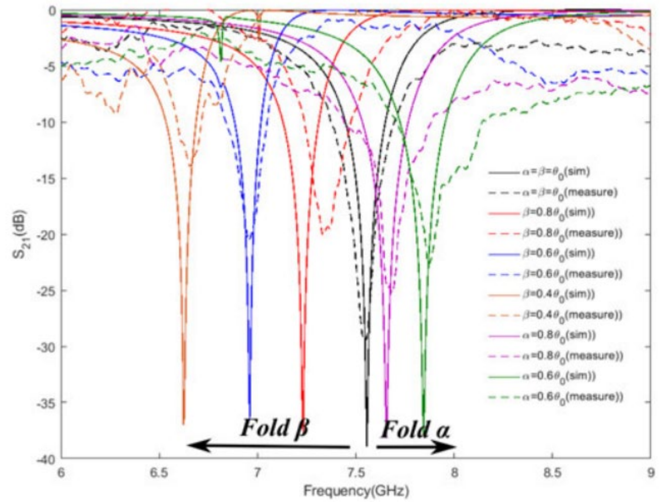


Horizontal (x-axis) polarization with different folding angles

- Cross-shaped dipole FSS element shows enhanced bandwidth, support for orthogonal linear polarization and ease of fabrication.
- 25% frequency tunable range over two polarization directions

Cui Y, Bahr R, Rijs SV, Tentzeris M (2021). A novel 4-DOF wide-range tunable frequency selective surface using an origami “eggbox” structure. International Journal of Microwave and Wireless Technologies 13, 727–733.

# 3D printed Liquid-metal-alloy microfluidics-based Zigzag and Helical Antennas for Origami Reconfigurable Antenna "Trees"

- "Tree" (zigzag/helical antenna) with dual-band (3GHz/5GHz) operability and different polarizations (linear/circular).
- Varying radiation patterns with "tree" compression.

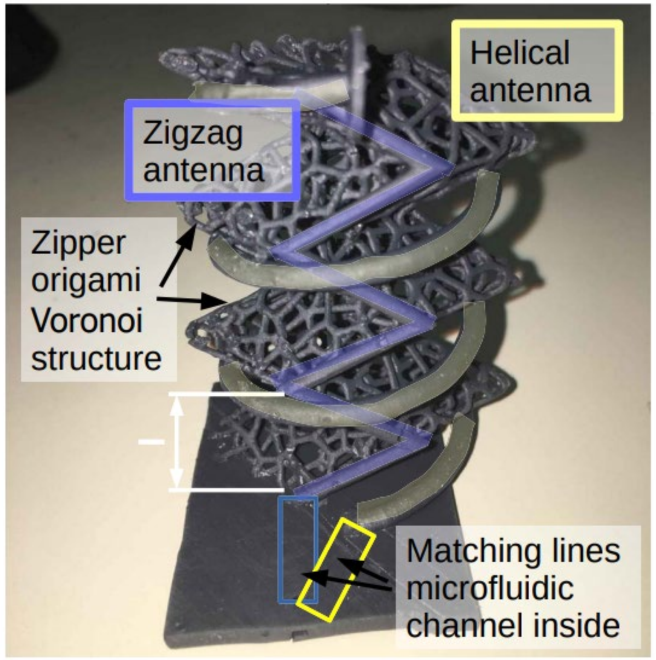


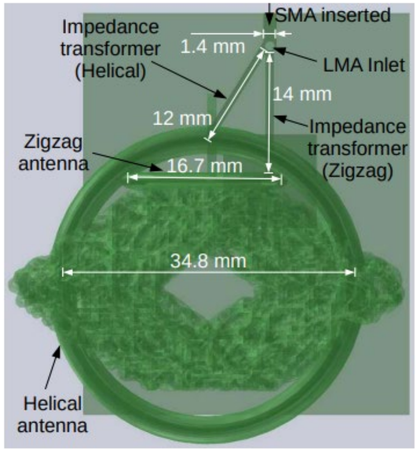


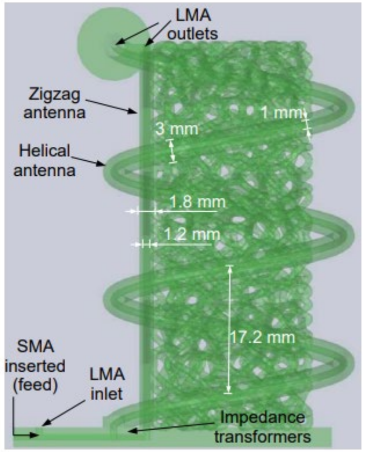


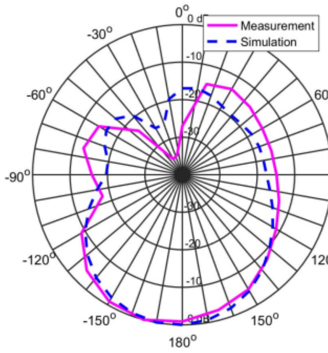


Original
(5 GHz)

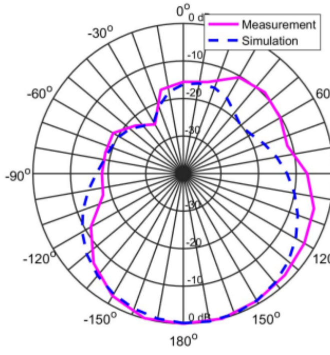


Compressed
(5 GHz)

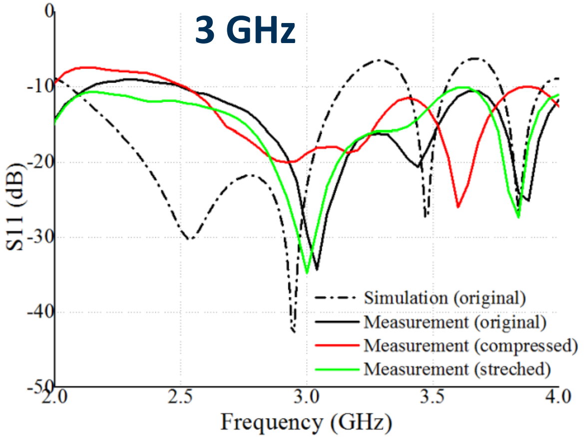


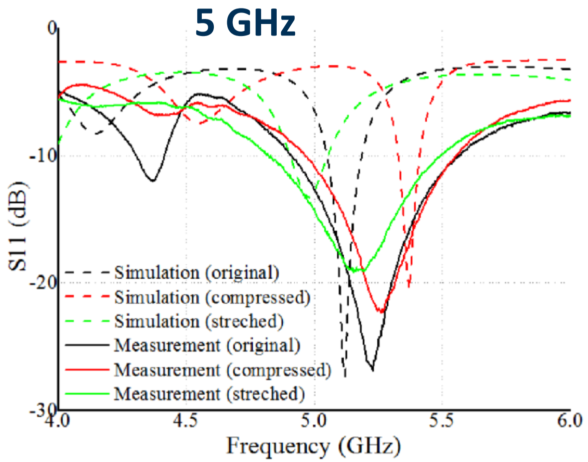


Su, W., Nauroze, S. A., Ryan, B., & Tentzeris, M. M. (2017, June). Novel 3D printed liquid-metal-alloy microfluidics-based zigzag and helical antennas for origami reconfigurable antenna "trees". In 2017 IEEE MTT-S International Microwave Symposium (IMS) (pp. 1579-1582).

# 3D Printed "Kirigami"-Inspired Deployable Bi-Focal Beam-Scanning Dielectric Reflectarray Antenna for mm-Wave Applications

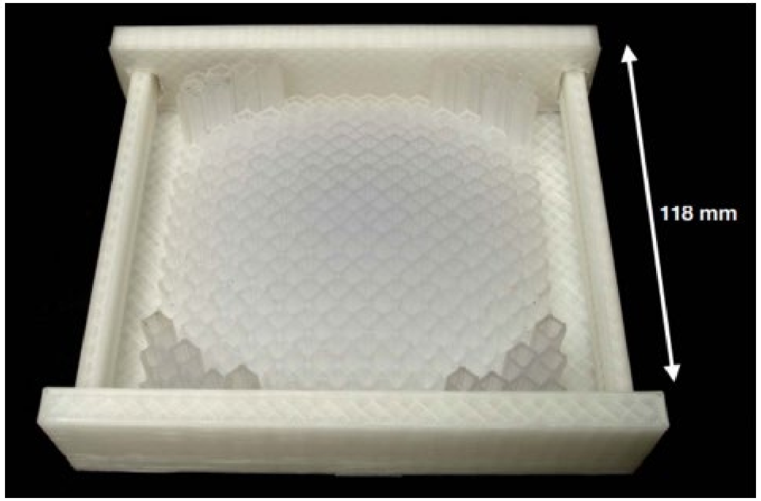


**Fully Deployed** (front side)


**Fully Retracted** (back side)

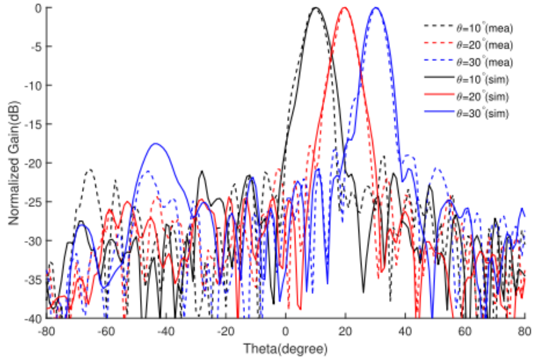


Radiation pattern at 30GHz with the scan angles from 10° —30°

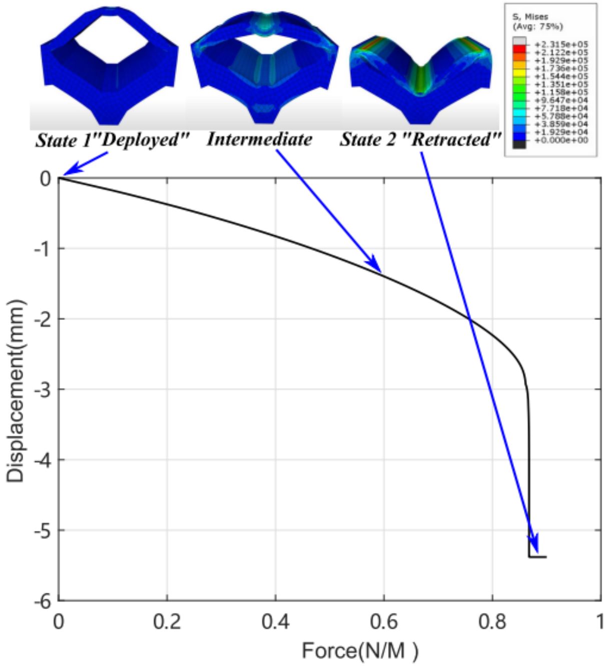


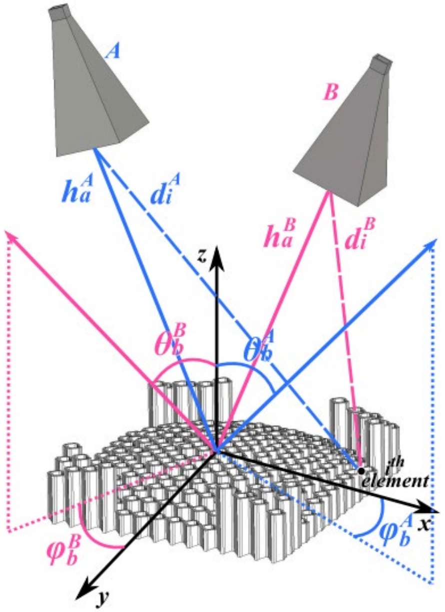


Bifocal beam scanning reflectarray setup

- Design enabled by a series of a "Kirigami"-inspired two-stage snapping-like element structure.
- Can be retracted by **66% to save space**.
- Bifocal phase distribution method is utilized to optimize performance of the array.
- Realized -30 ° to -10° and 10° to 30° beam-scanning ability.

Y. Cui, R. Bahr, S. A. Nauroze, T. Cheng, T. S. Almoneef and M. M. Tentzeris, "3D Printed "Kirigami"-Inspired Deployable Bi-Focal Beam-Scanning Dielectric Reflectarray Antenna for mm-Wave Applications," in IEEE Transactions on Antennas and Propagation, vol. 70, no. 9, pp. 7683-7690, Sept. 2022.

# 4D Printed Origami-inspired Tunable Multi-layer Frequency Selective Surface

- Fully additive hybrid (3D and inkjet) printing processes to realize a flexible two-layer substrate with conductive traces on both top and bottom.
- Significant strength improvement over paper-based origami structures.
- “Morphing" design that would be otherwise difficult to fabricate using traditional paper-based substrates
- Operability in mm-wave frequencies up to at least 28 GHz.

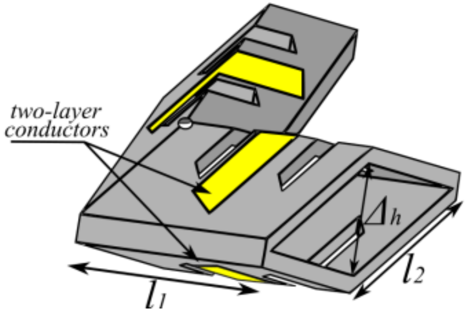


Mirror stacked multi-layer Miura FSS element

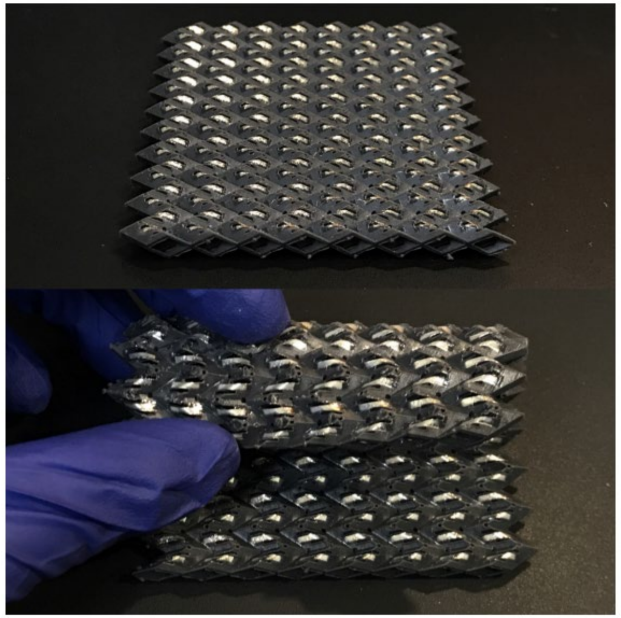

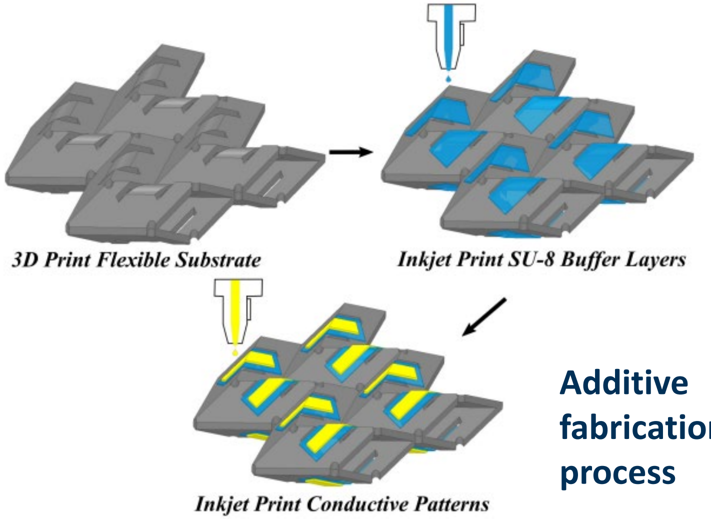


**Additive fabrication process**

Different **folding angles**

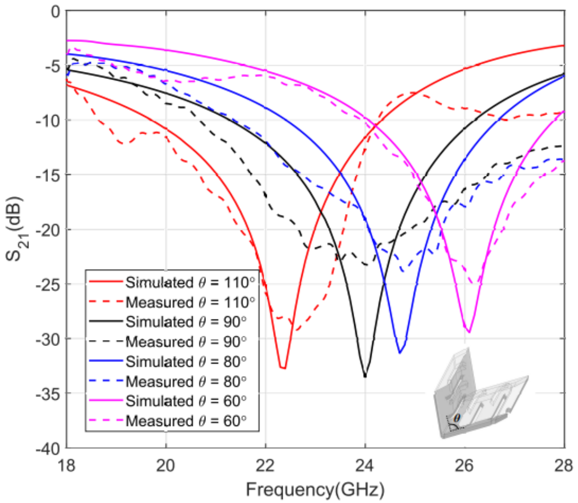


Different **incident angles**

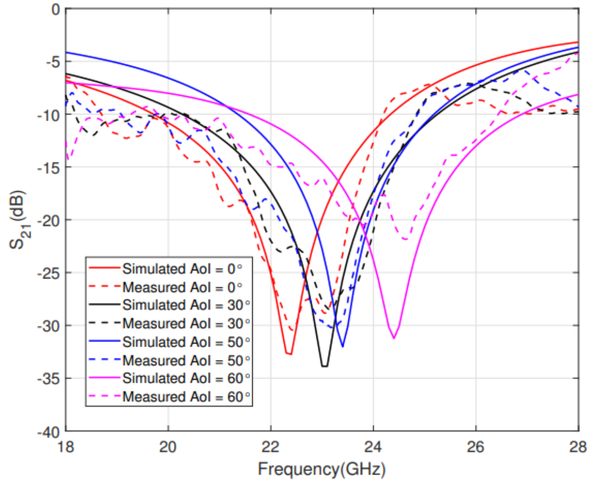


Cui, Yepu, et al. "A Novel Additively 4D Printed Origami-inspired Tunable Multi-layer Frequency Selective Surface for mm-Wave IoT, RFID, WSN, 5G, and Smart City Applications." 2021 IEEE MTT-S International Microwave Symposium (IMS). IEEE, 2021.

# Hybrid Printed Electromagnetic Pressure Sensor using Metamaterial Absorber

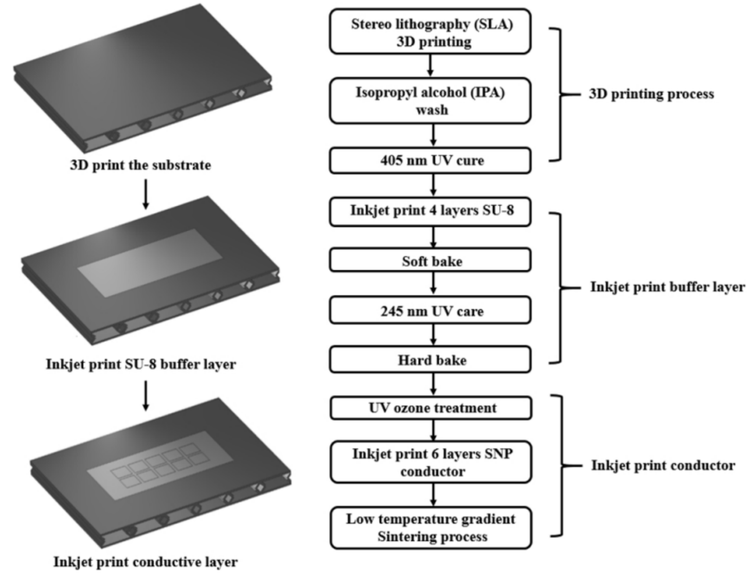


**Fig. 5.** Fabrication process for the proposed hybrid (3D and inkjet) printed EM sensor.

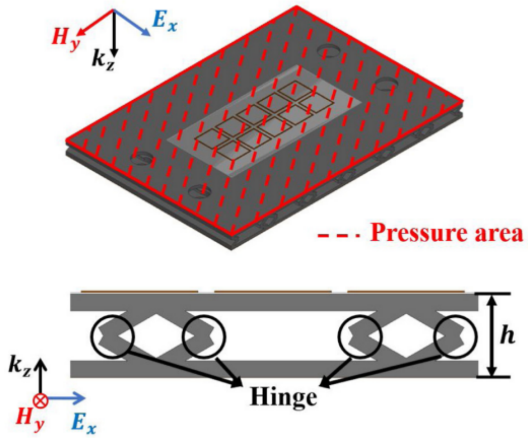


**Pressure area and hinges**

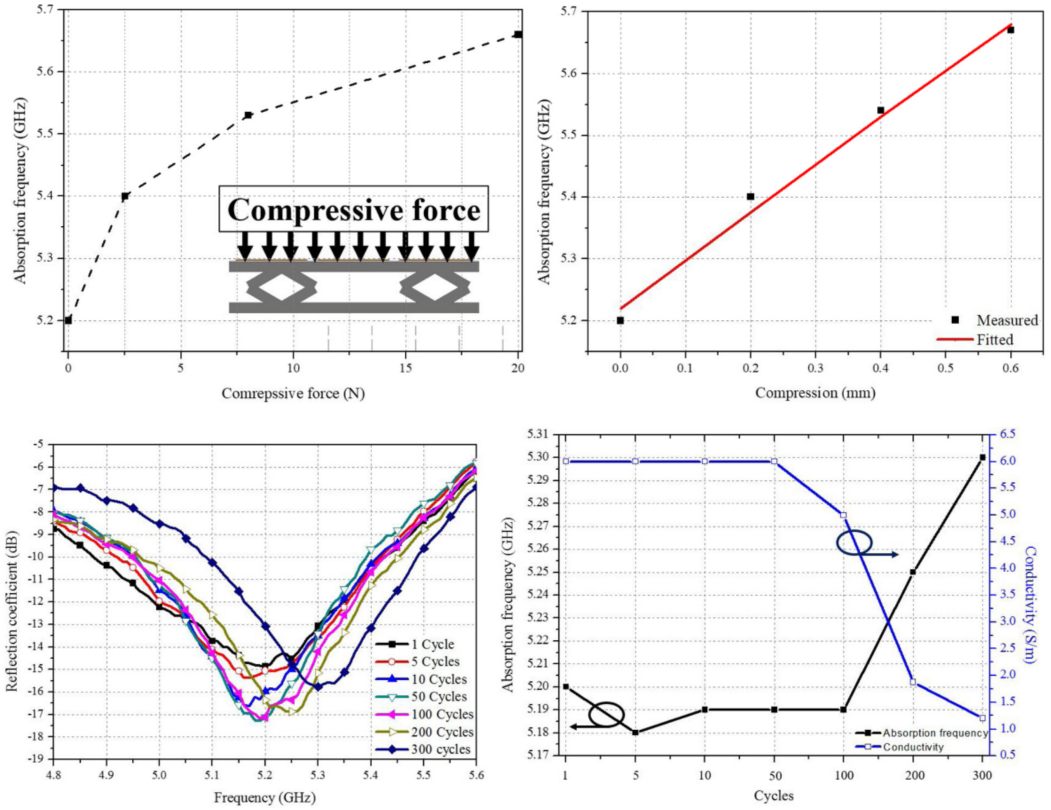



(a) (b)

**Fig. 7.** Fabricated electromagnetic pressure sensor prototype (a) top and (b) side view.

Heijun Jeong, Yepu Cui, Manos M. Tentzeris, Sungjoon Lim, Hybrid (3D and inkjet) printed electromagnetic pressure sensor using metamaterial absorber, Additive Manufacturing,Volume 35,2020,101405,ISSN 2214-8604

- Absorption frequency varied with substrate thickness: electromagnetic pressure sensor with mechanically transformable substrate.
- Absorption frequency 5.2 to 5.66 GHz by applying 0 and 20 N pressure; device sensitivity = 7.75 × 10^8 Hz/mm (0.2 × 10^8 Hz/ N); and repeatability was retained up to 100 cycles.

# Artificial Intelligence: the key enabler

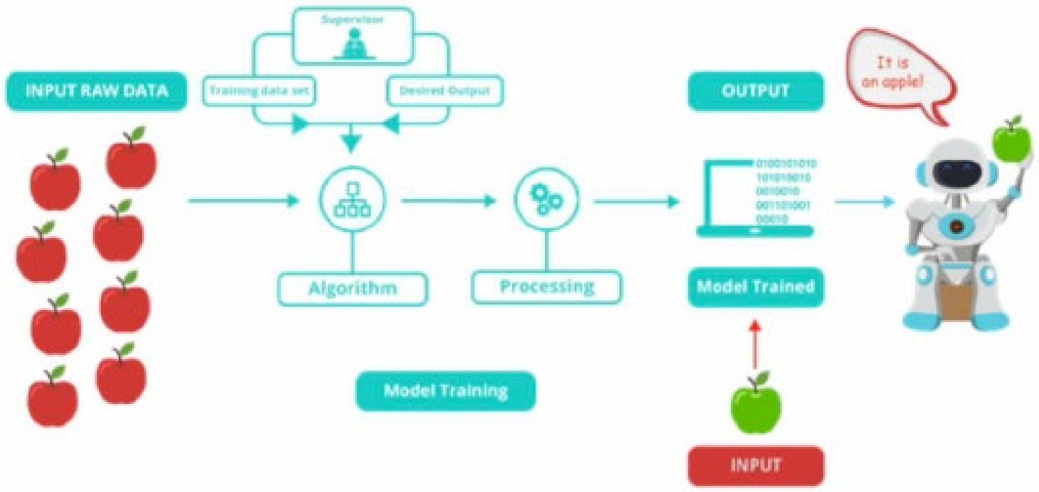


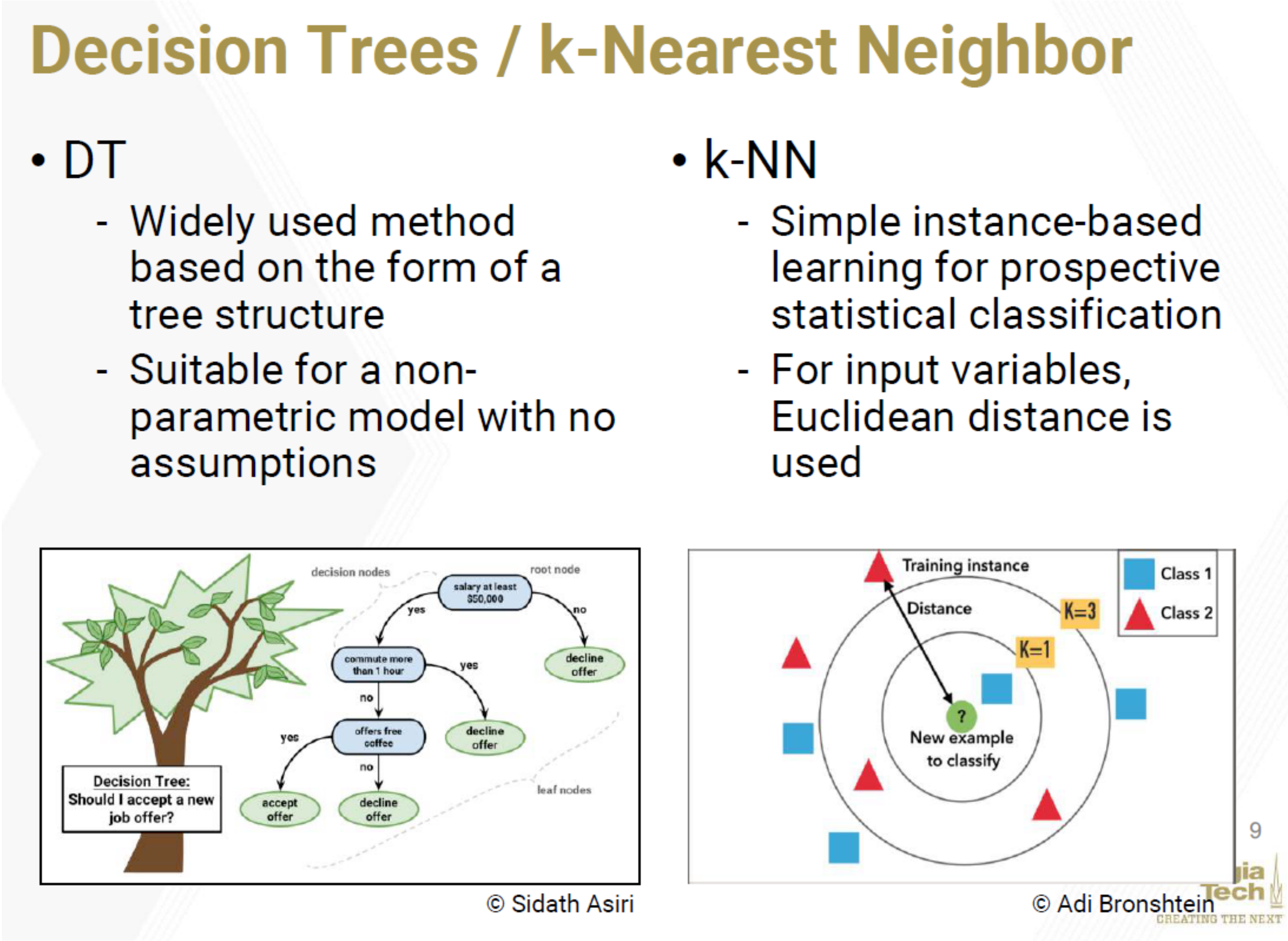

# Machine Learning-Enhanced mmID-"Gyro" for 3-Axis Orientation Wireless Detection

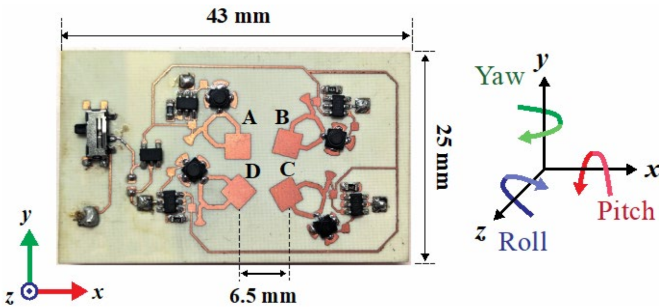


✓ Low Cost mmWave System

- Ultra-low-power, sticker-like mmWave mmID
- Comprised of four backscattering elements that are multiplexed in amplitude, frequency, and spatial domains
- Each element designed with polarization offset of 15° from each other to allow for angle of rotation encoding
- Cross Polarization antenna configuration utilized to reduce signal interference to reader
- 24 GHz FMCW Radar utilized as reader

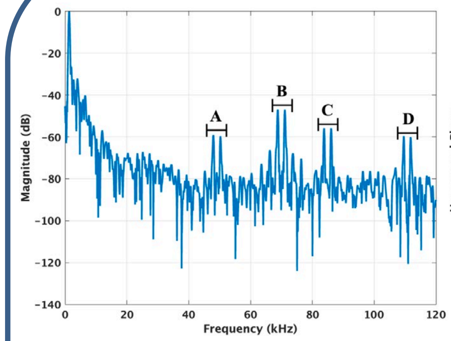


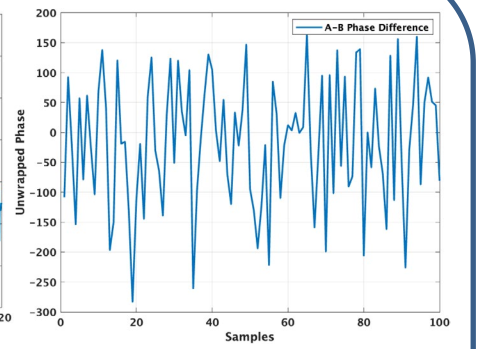


✓ Digital Signal Processing

- Amplitude Response of each antenna element
- Phase Difference of neighboring elements using Arctangent Demodulation Algorithm

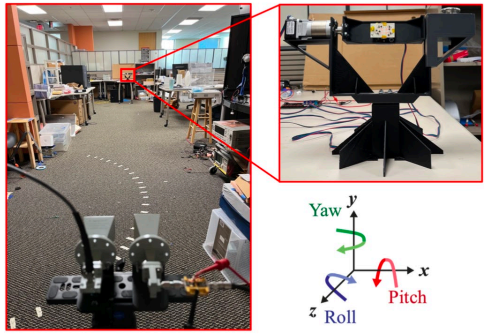


✓ Data Processing/Machine Learning

- Tag rotated over ± 90°, with increments of 10°, in each axis
- K-Nearest Neighbors (KNN) Algorithm
- Global Dataset of 2.8 million data samples
- 80/20 Train-Test Split

| Range | Model A | Model B |
|---|---|---|
| 0.5 m | 99.60% | 99.87% |
| 1 m | 95.59% | 99.85% |
| 2 m | 81.19% | 99.77% |
| 3 m | 67.29% | 98.67% |
| 4 m | 58.81% | 97.95% |
| 5 m | 53.29% | 93.73% |
| 6 m | 47.14% | 91.36% |
| 7 m | 46.45% | 88.51% |
| 8 m | 45.89% | 85.43% |
| 9 m | 45.22% | 82.19% |
| 10 m | 45.01% | 77.88% |

✓ Results

- 2 Models trained
  - Model A: Only Amplitude Response
  - Model B: Amplitude Response and Phase Difference
- Accuracy >91% achieved at up to 6 m with Model B
- Further evaluation to be performed with a finer angular resolution for an even more precise orientation detection

# Self-Calibrated “Flex-compensating” Flexible Arrays

- Conformal applications of arrays allows for superior integration in wearables, aerospace and communication platforms.
- However, phase error causes gain degradation -> Needs Correcting

Requires a way to adaptively know the current bending condition in order to accurately correct for bending

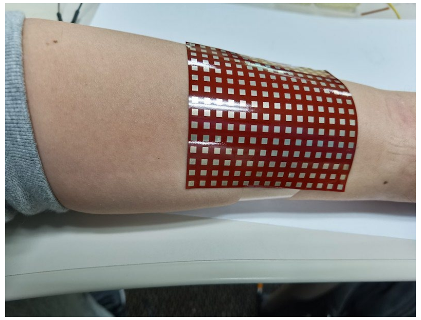

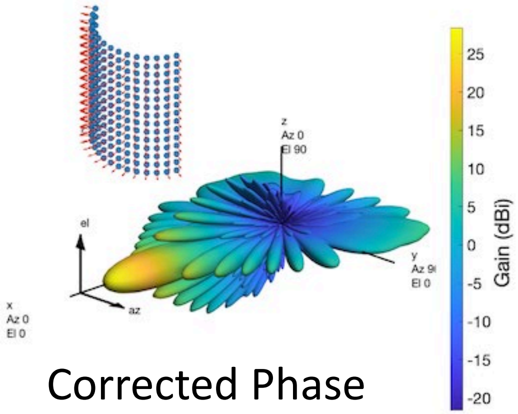


Corrected Phase

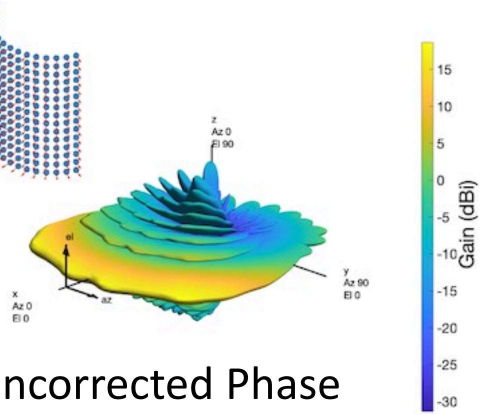


Uncorrected Phase

90% accuracy and only 0.071dB in gain error

# Fully Printable Tile-by-Tile Reconfigurable Intelligent Surfaces

- Independent **beam-steerable** flexible planar TX and RX antenna array systems
- Frontend ICs with built-in phase shifters to steer the array of each tile, with **individually controlled radiating element**
- Corporate feed network connects **removable tiles** to build a larger array
- **Flexible tiles and feeding network** can be conformally wrapped around curved surface

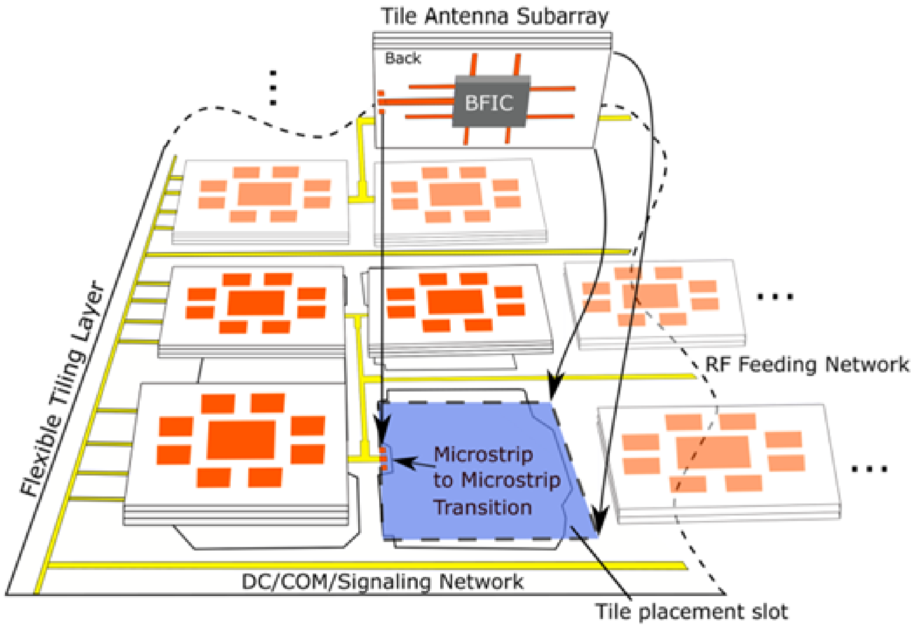


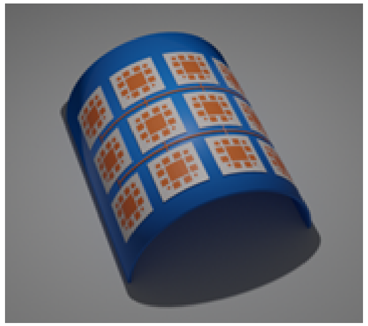

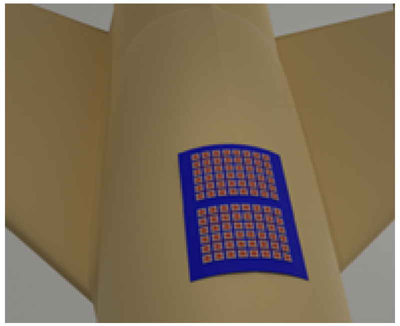

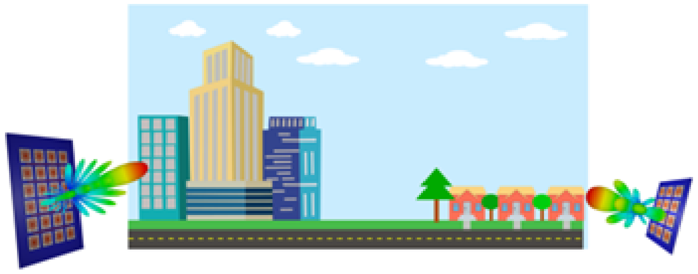

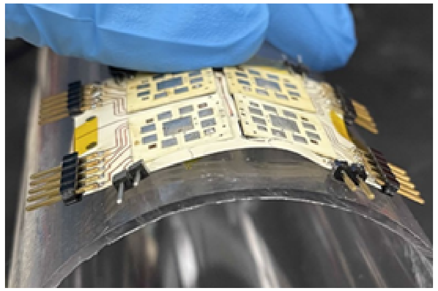

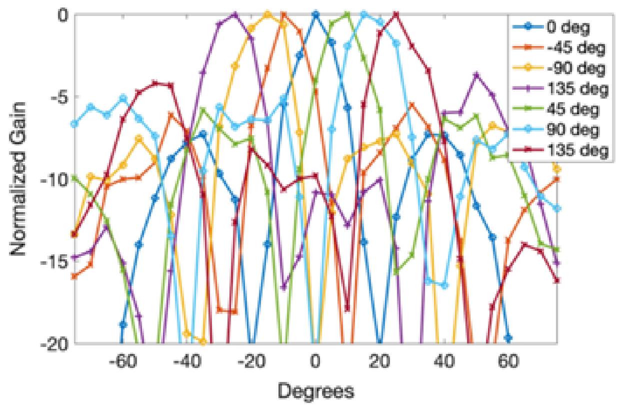

# Computer Vision Aided Calibration of Tile-Based Phased Arrays

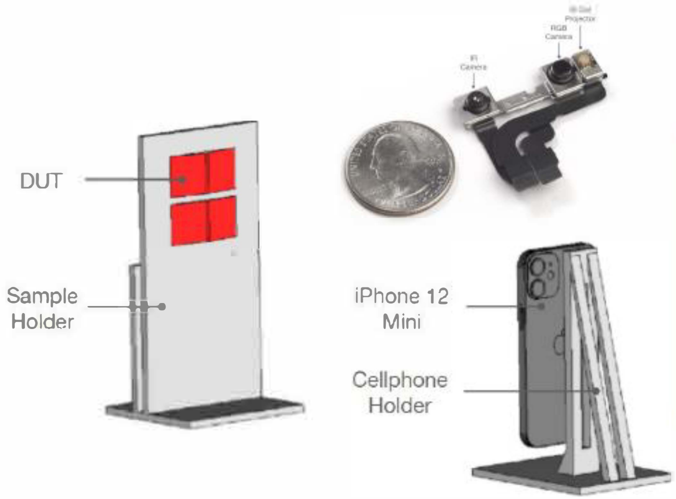


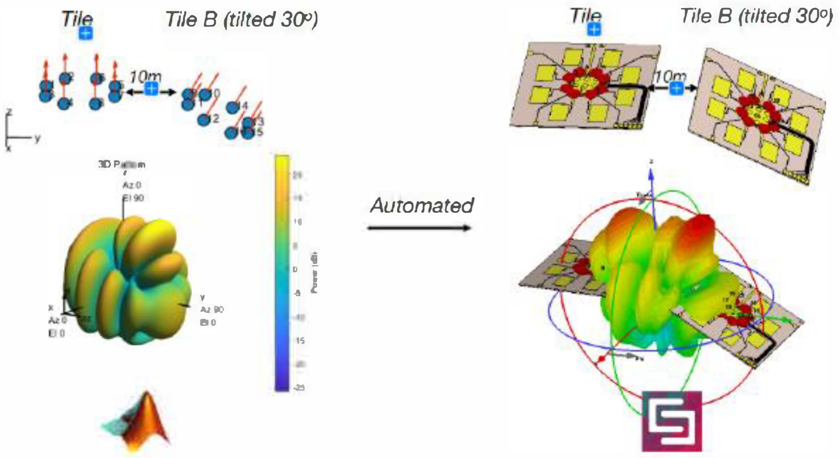


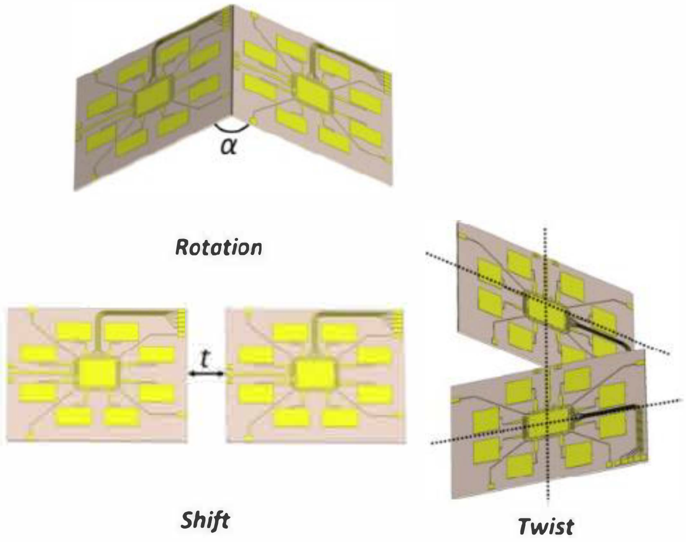


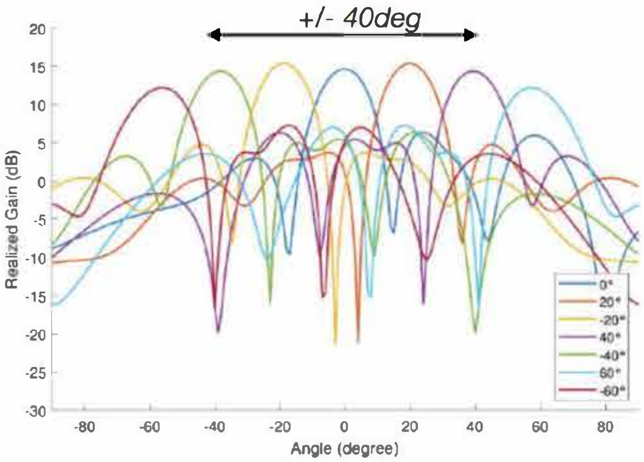


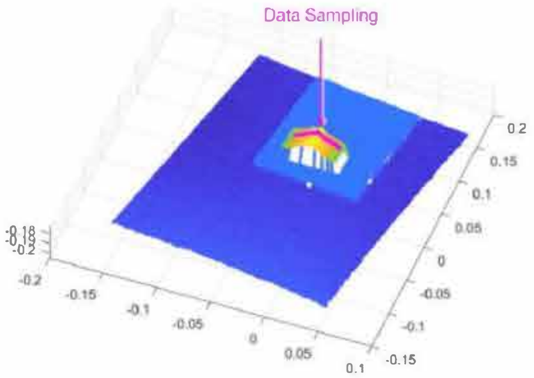


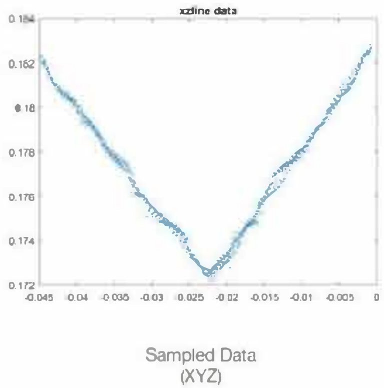


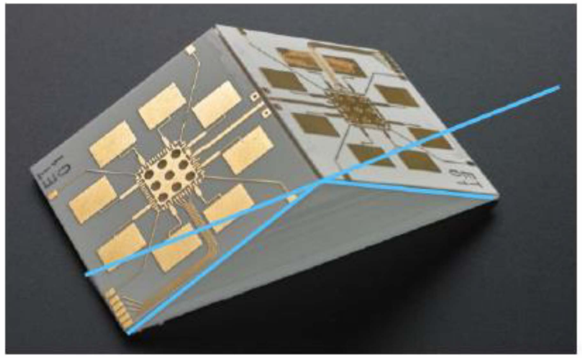

# The Internet of Smart Skins

- Thin, Flexible device: the Skin
- Ultra-low-power: <20 μW
- Battery-less: Energy Harvesting
- Long-range: 250m+
- Localizable in real time (**cm accuracy**): single-reader localization (Angle+range)
- Metal-mounting compatible
- Enhanced by 5G+/6G.

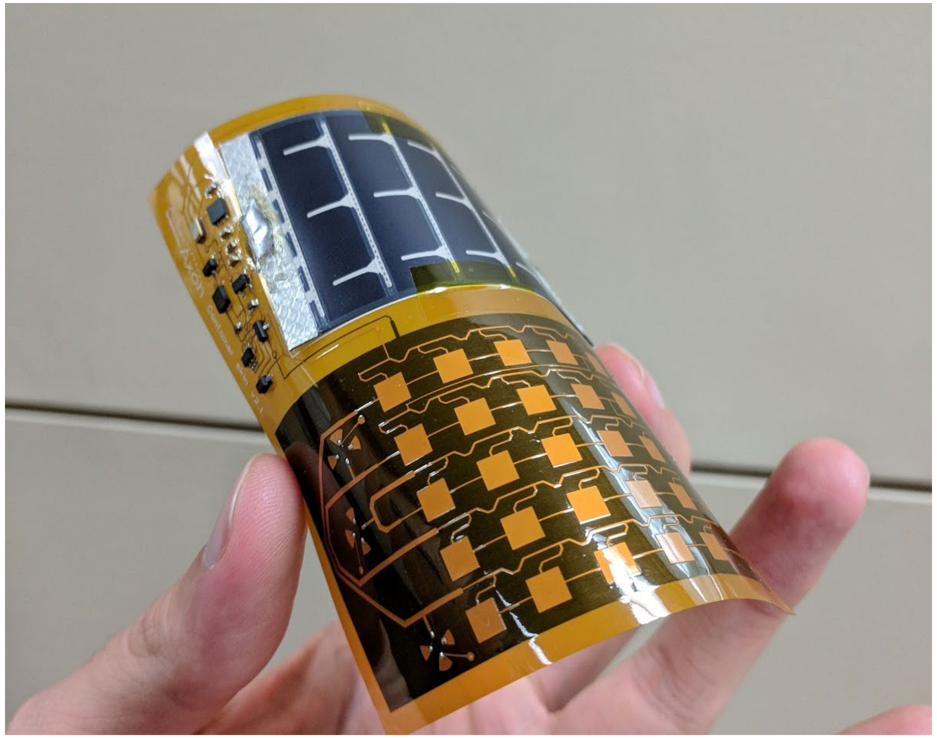

[5S *Challenge: Smart-Scalable-Sustainable-Speedy-Secure]*

# Wireless Charging of UAV constellations/Wireless Sensor Modules Using 5G / 5G as a Wireless Grid

## How does it work

*Dual Combination: RF + DC*

### Scavenge mm-Wave Signals

STEP 01

Antenna arrays connected to the antenna ports of the Rotman lens scavenge the mm-wave energy from all directions.

### RF Combine and Focus

STEP 02

The Rotman lens combines internally all the mm-wave signals collected by the antennas and focuses them to one beam port on the opposite side, where a rectifier is connected.

### Rectify and DC Combine

STEP 03

The rectifiers connected at the beam ports of the Rotman lens convert the mm-wave energy to DC power. The DC combiner enables an efficient voltage extraction irrespective of the direction of the incoming signal.

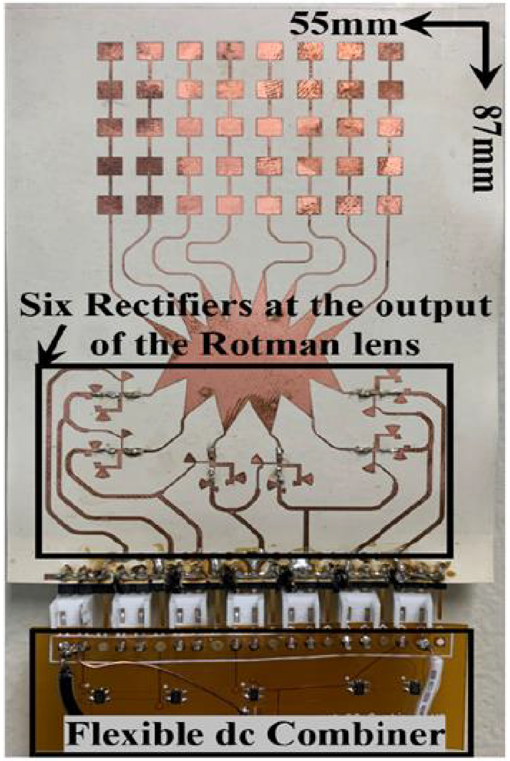



scientific reports

OPEN 5G as a wireless power grid

# Wireless Charging of UAV constellations/Wireless Sensor Modules Using 5G / 5G as a Wireless Grid

## Rotman Lens for mm-wave harvesting

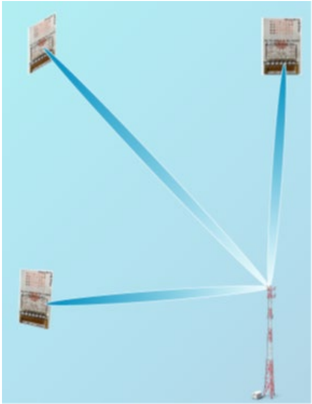

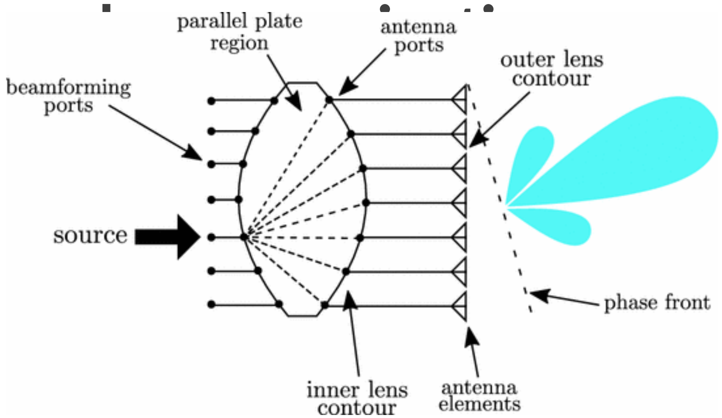


***Breaking the High Gain and Large Beamwidth Trade-off at mm-Wave Frequencies***

- Electrically large antennas
- High gain and lack of isotropic behavior
- Use of BFNs

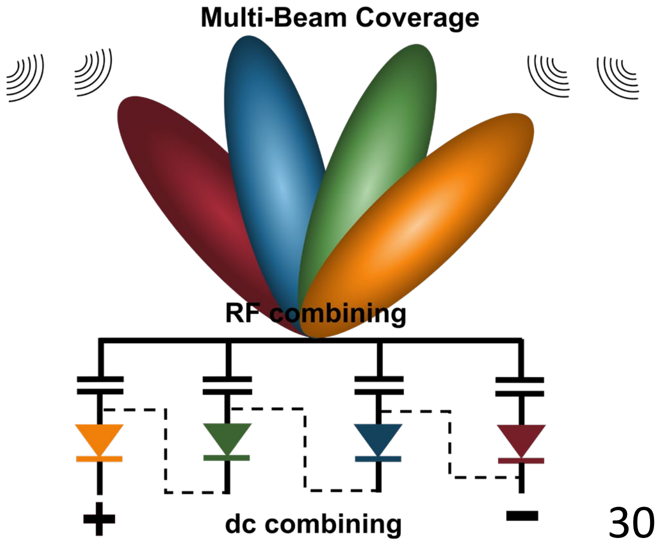


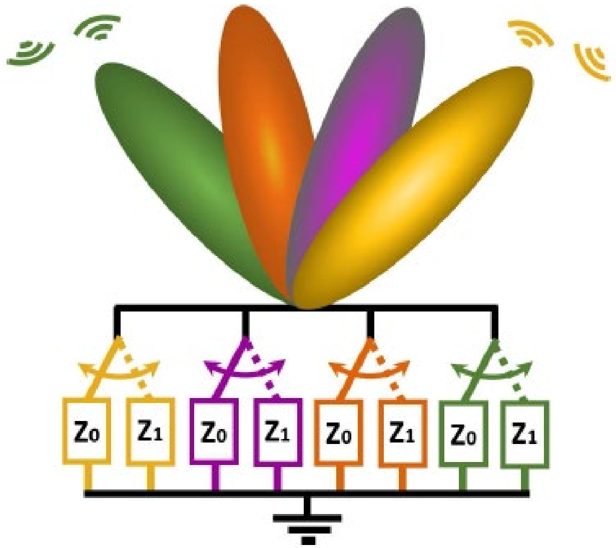

# Wireless Charging of UAV constellations/Wireless Sensor Modules Using 5G / 5G as a Wireless Grid

## Scalable and Broadband Structure

Optimal compromise (Na=8, Nb=6):

- High array factor of 5.95 dB
- 120◦ total angular coverage

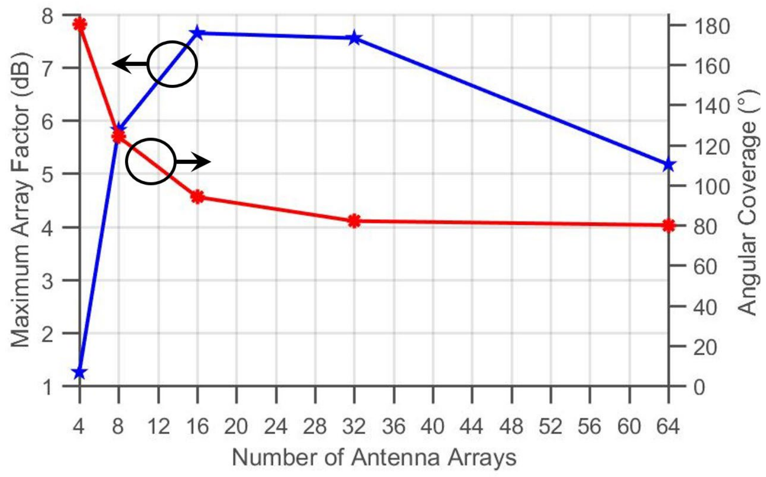


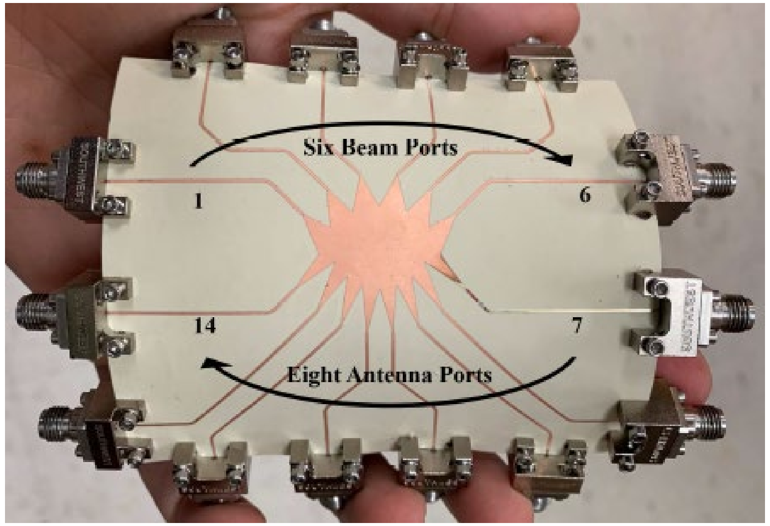


*P1, P6: Edge Beams*

*P2, P5: Secondary Beams*

*P3, P4: Center Beams*

- Beamwidth and array factor maintained over a large bandwidth exceeding 20 GHz

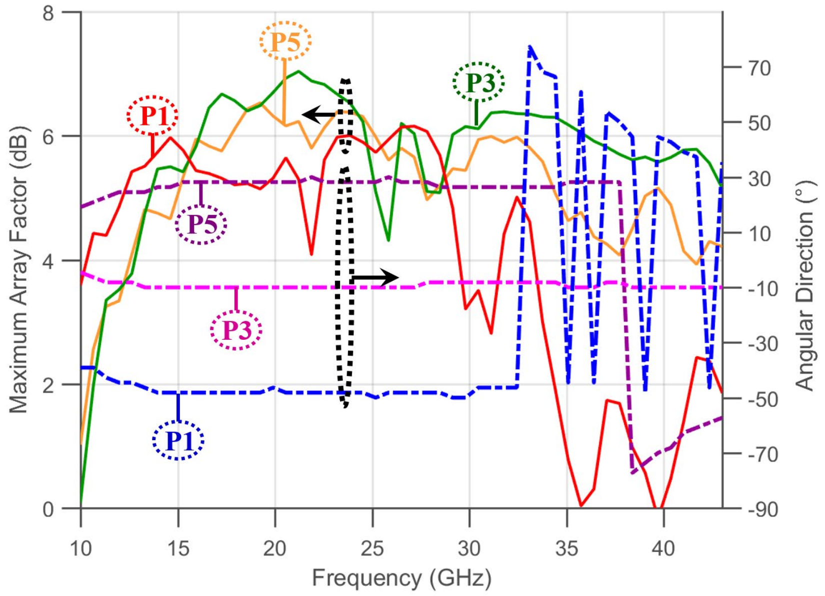

# Breaking the trade-off

- Eight serially-fed patch antenna arrays added
- Simultaneous 17dBi gain and 110° angular coverage at 28GHz
- Minor gain deterioration under severe bending

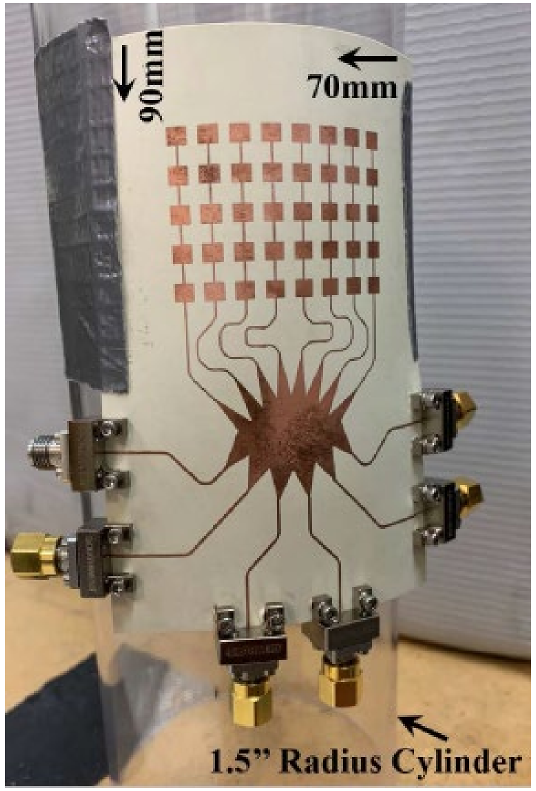


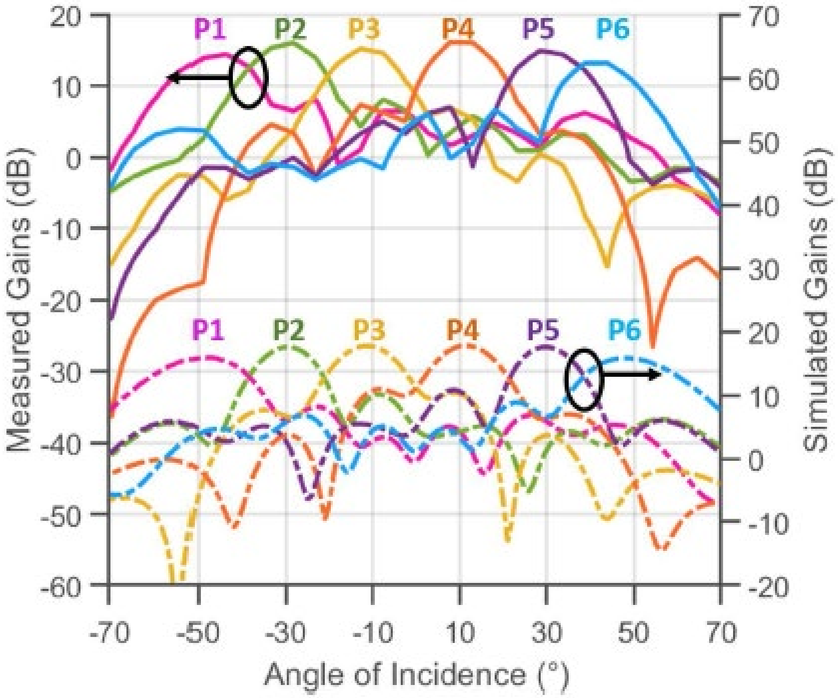


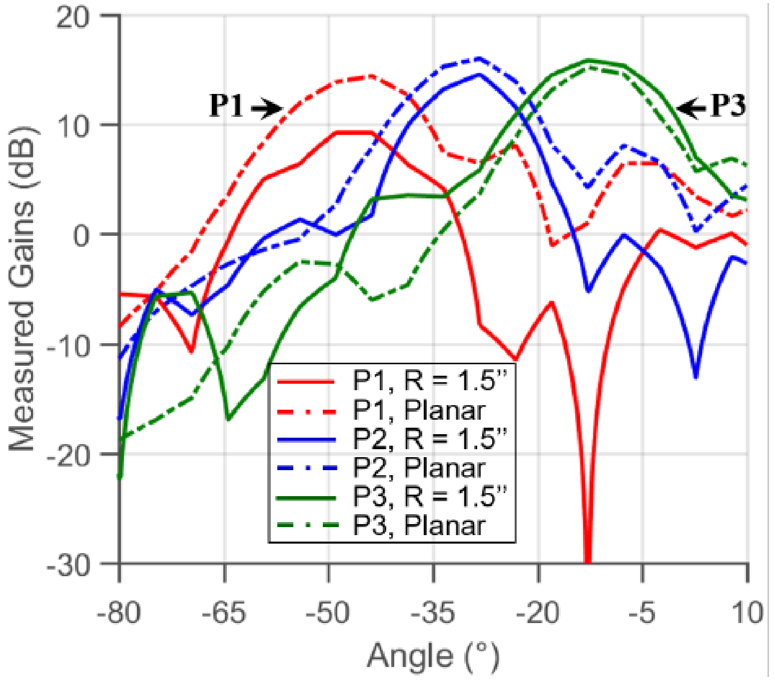

# Rotman-Lens-Based Reconfigurable Intelligence Surface mmID with Energy Harvesting Capability 5G+

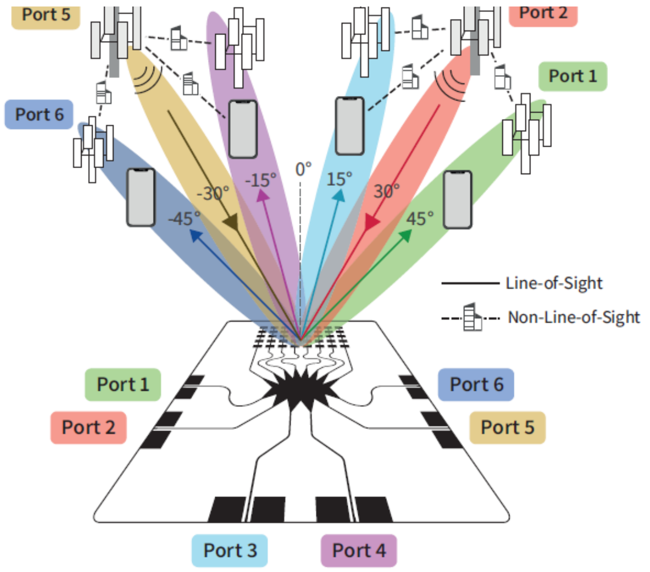


Fig. 1. Rotman lens antenna array beaming diagram in complex urb environment.

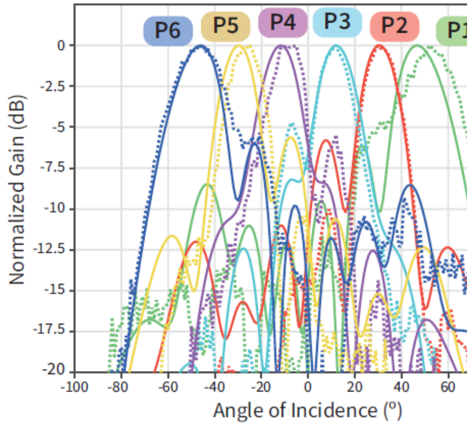


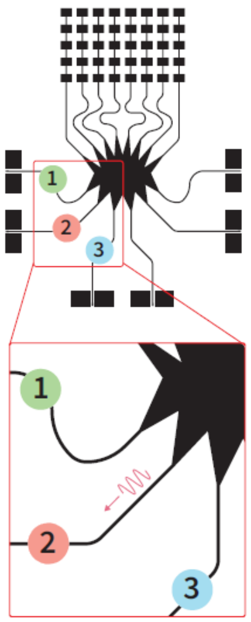


(a) Rotman Lens Port Layout

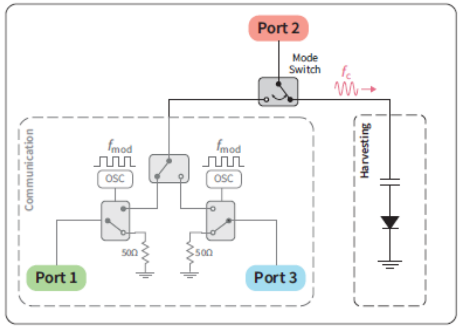


(b) RIS Design Harvesting Mode

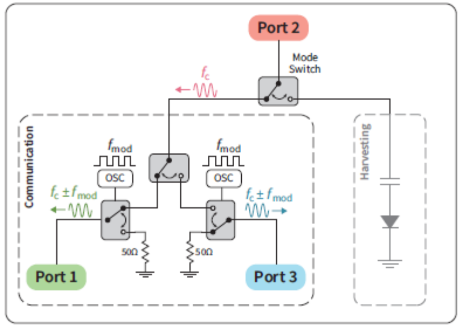


(c) RIS Design Communication Mode

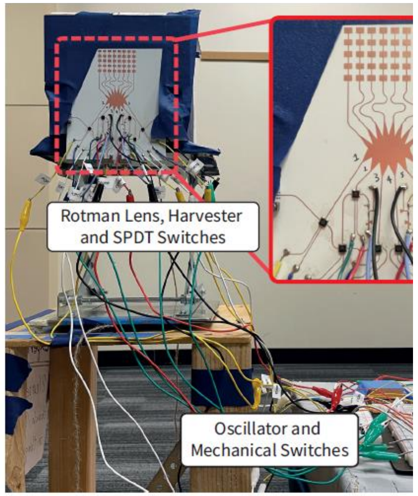


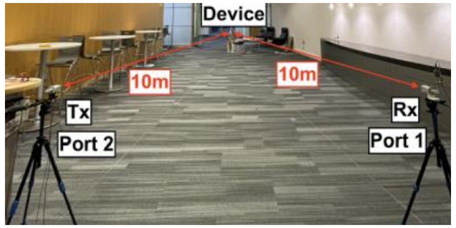


- Reconfigurability by 8uW switches , low power oscillator is used to provide ASK modulation to the signal.
- Addressed NLOS challenge in RIS
- 2.5dBm turn-on power, harvest 28GHz 11m away and communicate 125m with 75dBm EIRP

# "Zero-Power" mmWave Smart Skins for Structural Health Monitoring

- Capability to detect cracks and <20 u-strain
- Range extended to 10 meters  through the use of Solar Power

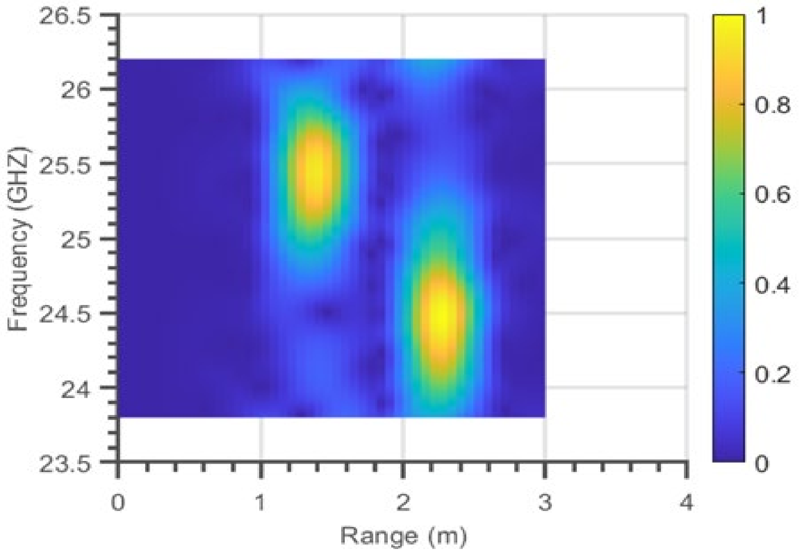


Frequency multiplexing allows dense implementation and discrimination in range

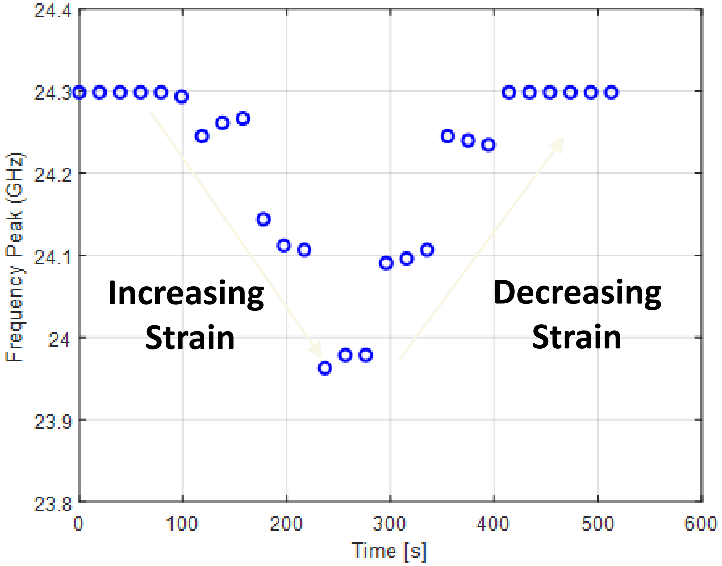


Sensor able to capture strain profile while embedded in composite material

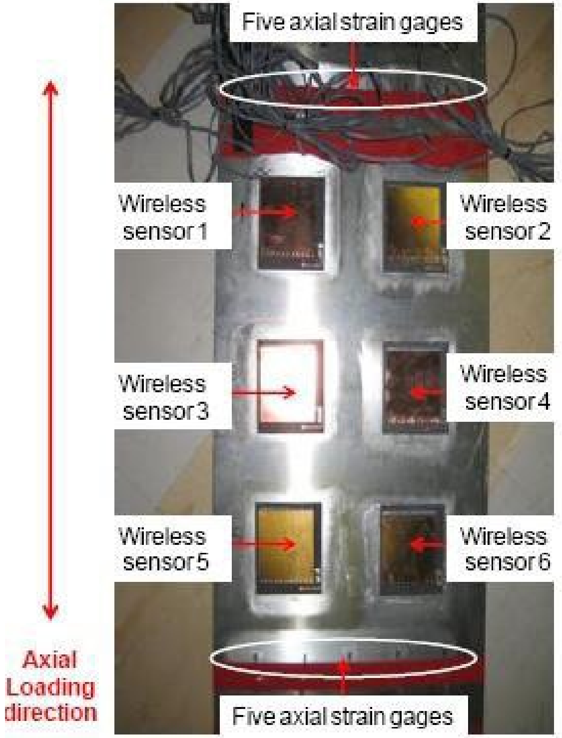


(a) Sensor instrumentation on the aluminum specimen

# Sensor Highlights in ATHENA Lab

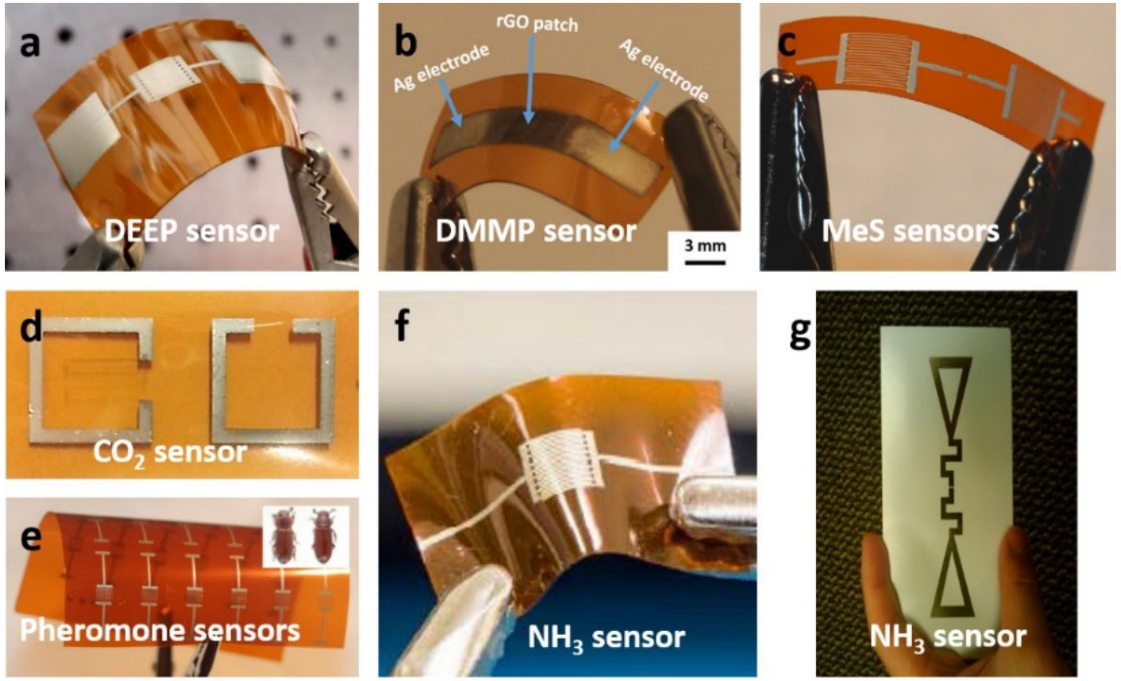


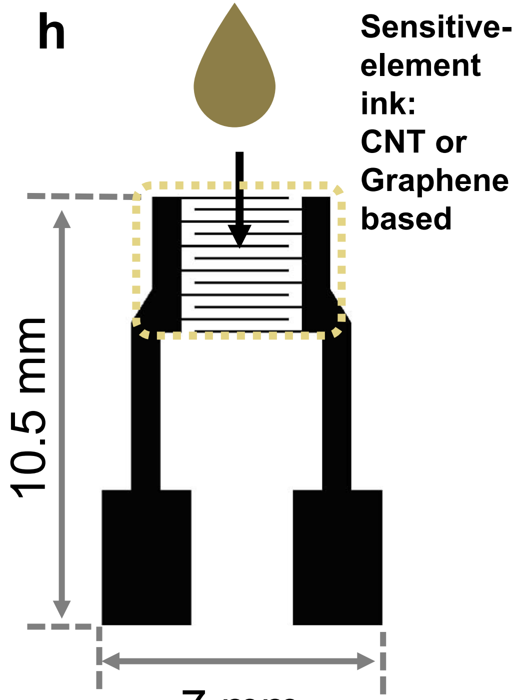


(a) Chemical warfare nerve agent simulant diethyl ethylphosphonate (DEEP)
(b) Chemical warfare nerve agent simulant dimethyl methylphosphonate (DMMP).
(c) Chemical warfare blister agent simulant methyl salicylate.
(d) Resonator sensor for CO2.
(e) Sensors for the aggregation pheromone of flour beetles.
(f) - (g) Sensors for NH3.

(h) Interdigitated electrode design to increase surface area

- Sensitive element is deposited between fingers
- Composition on target analyte
- CNT functionalized with different molecules

# Wearable Inkjet-Printed CO2 Sensor

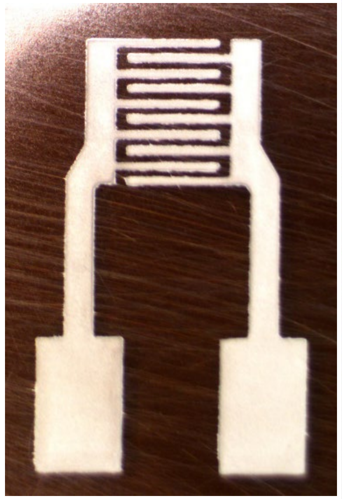

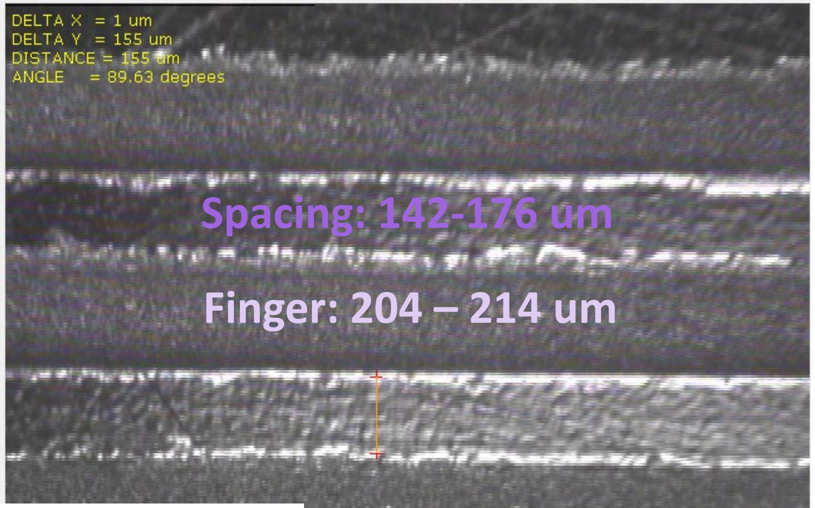


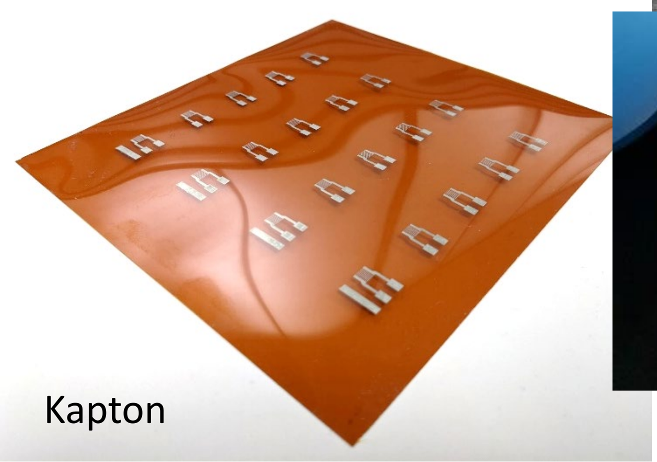


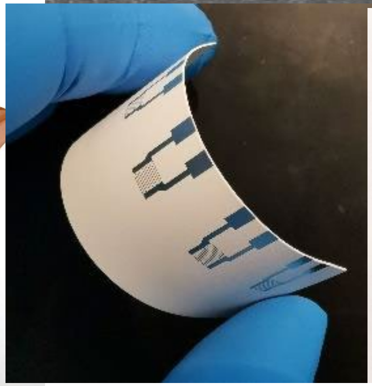

Other substrates:
Rogers, Teslin paper, FR4

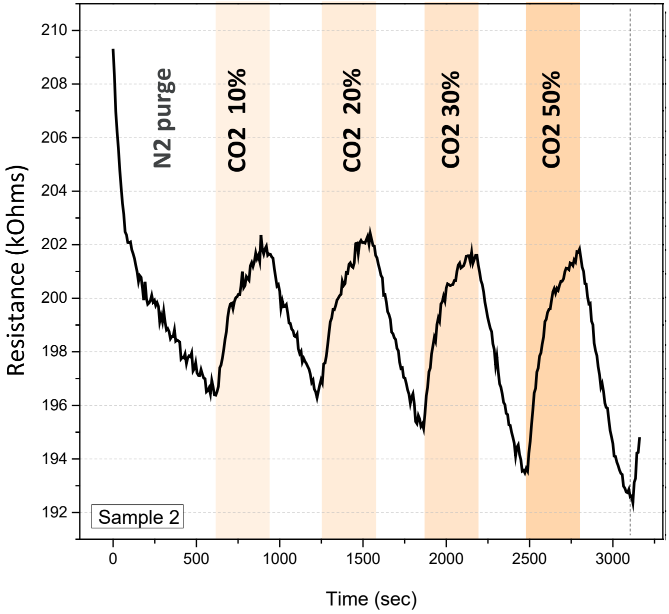


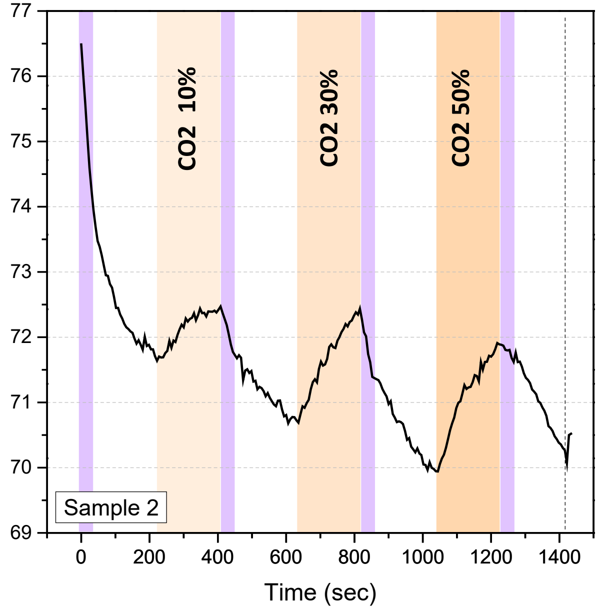


- Preliminary results on FR4 substrate
- Use of UV light to reduce recovery time
- Slope change due to different concentrations

# Printed Covid antibody sensors

Inkjet-printed electrode
On Teslin® paper

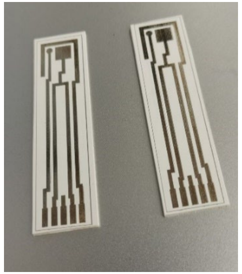

Inkjet-printed electrode
On Kapton® PI film

3D-printed
Electrode and coated
with rGO

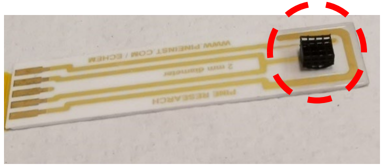

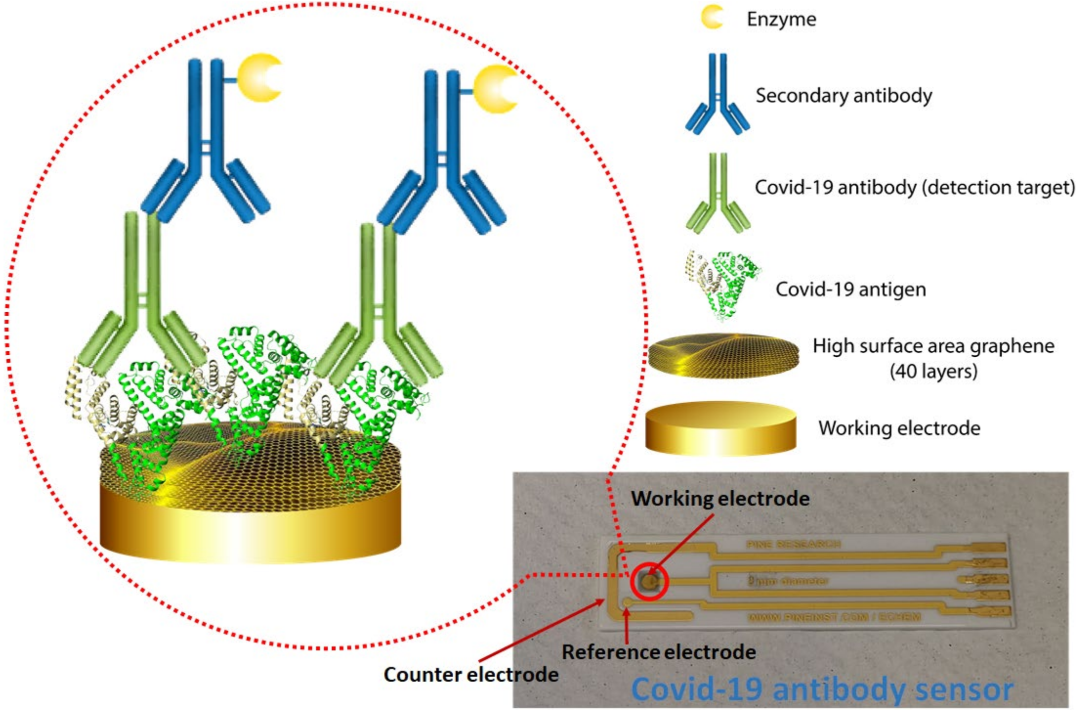


Commercial electrode

# Printed Covid antibody sensors

## Detection of both natural and synthetic Covid antibodies

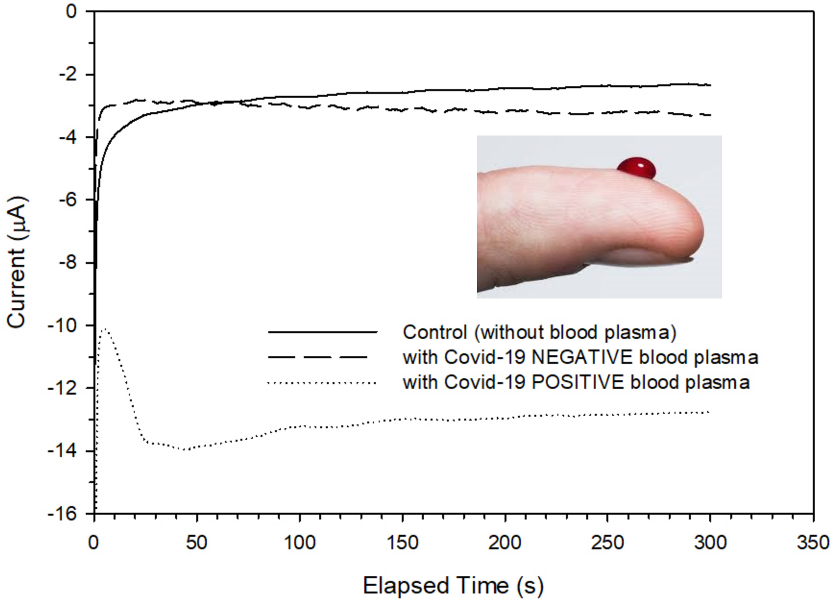


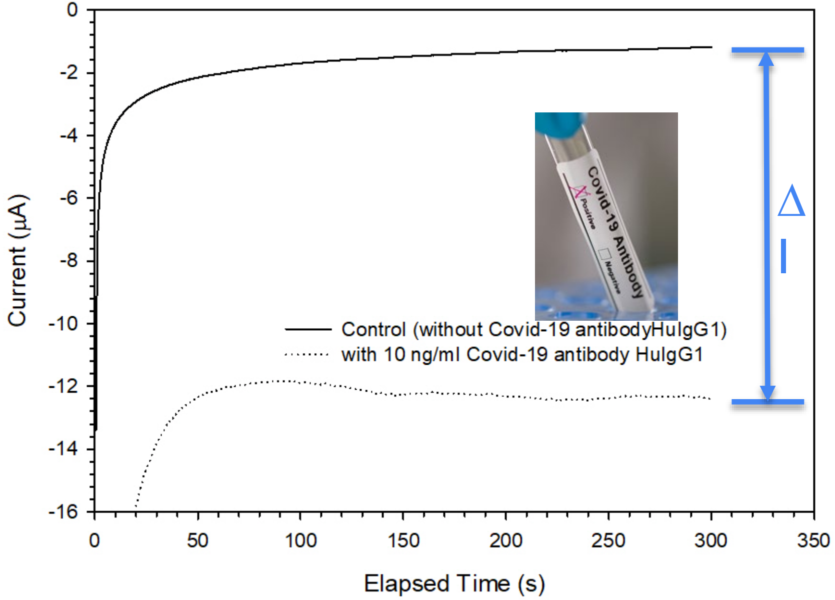


- **Clear differentiation between Covid -19 negative and positive blood samples**

# Zero-Power Environmentally-Friendly Self-Healing "Morphing" (4D) 5G+/mmW Fully-Additively Manufactured Platforms and Reconfigurable Intelligent Surfaces with "Smart Skin" Tile-by-Tile Sensing and Ultrawideband Frequency/Pol Reconfigurability

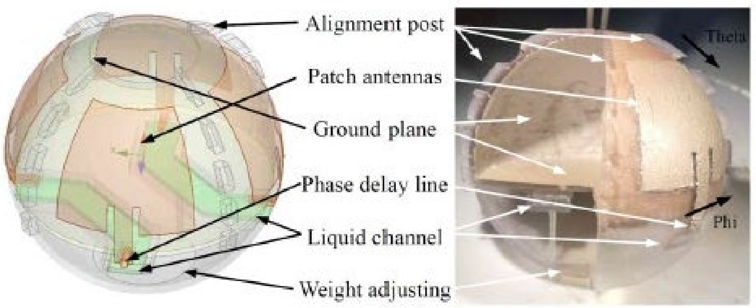


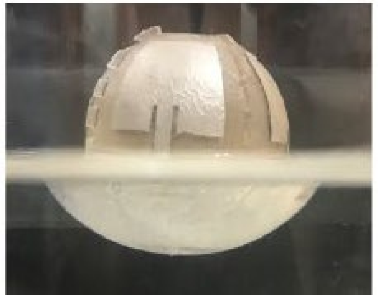

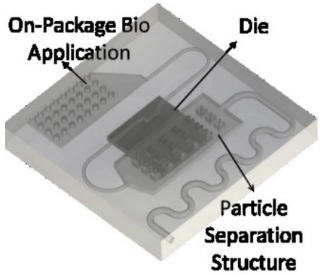


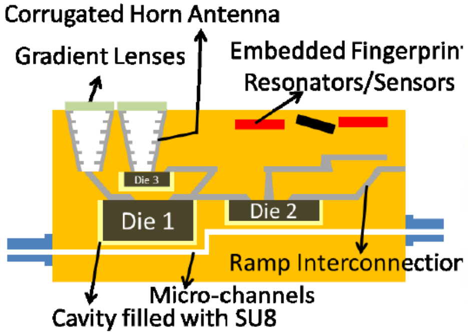


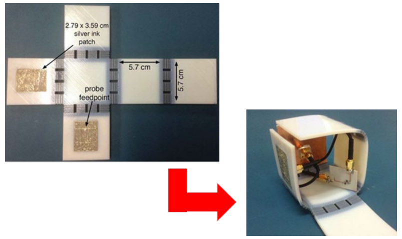

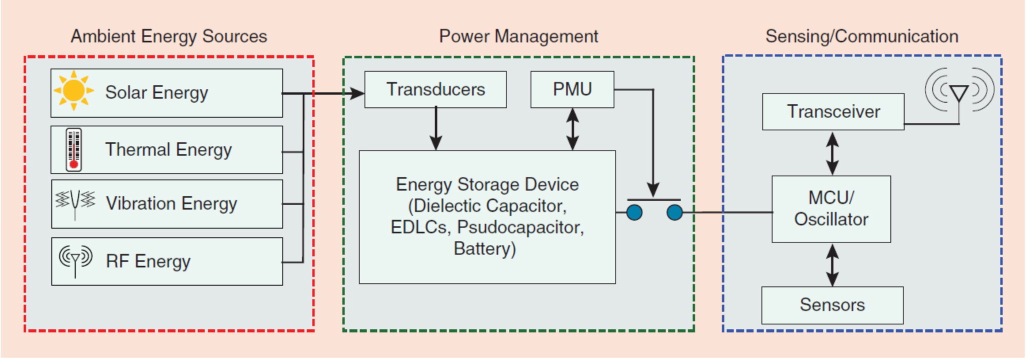


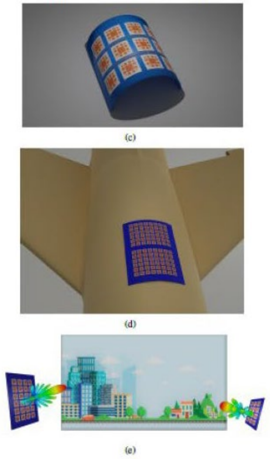


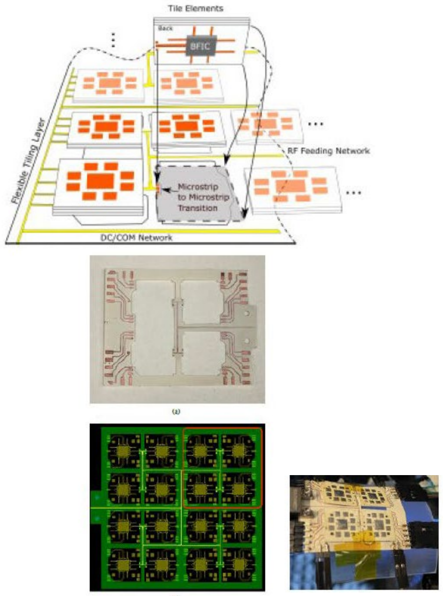


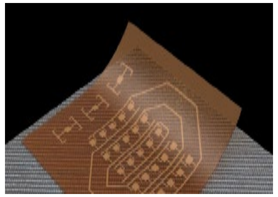

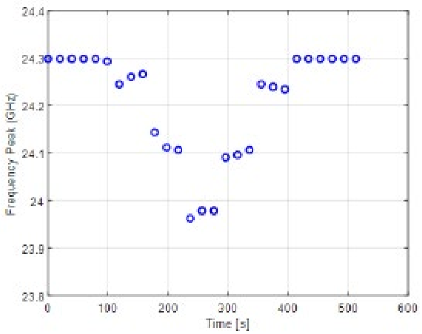


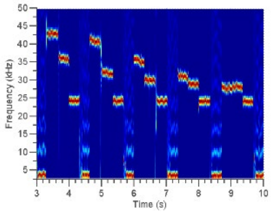


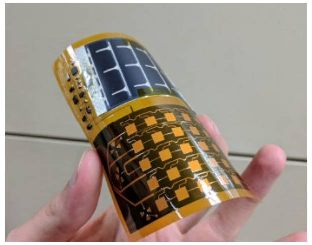

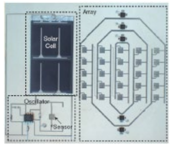

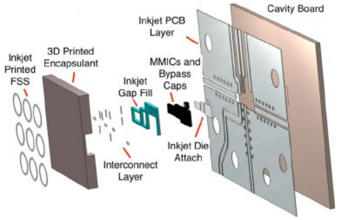


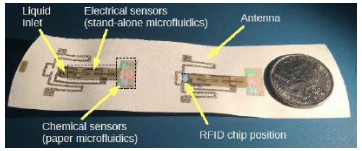


**Emmanouil Tentzeris**

tentzeris.ece.gatech.edu

000546

ATHENA Georgia Tech